Optimal N-state endogenous Markov-switching model for currency liquidity timing

Luqi Wang[a], Giovanni Urga[a,*]

[a] *Centre for Econometric Analysis and Faculty of Finance, Bayes Business School (formerly Cass), City St George's University of London, 106 Bunhil Row, EC1 8TZ, London (UK)*

Abstract

In this paper, we examine whether globally-diversified funds' actively adjust their currency exposure in response to systematic currency liquidity movements, a behavior we term *currency liquidity timing*. A novel currency-liquidity-timing model embedded with an N-state endogenous Markov-switching mechanism is proposed to capture the dynamics in funds' timing behavior, as well as the external and internal drivers influencing such dynamics. Using a sample of 382 international fixed income mutual funds from July 2001 to December 2020, we find evidence of currency liquidity timing at the aggregate level for the sample funds. Interestingly, funds' currency-liquidity-timing behavior exhibits a state-switching pattern across different market periods: funds on average engage in perverse currency liquidity timing during tranquil market periods, but in positive currency liquidity timing with a stronger degree of aggressivity during more turbulent market periods. Our results suggest that the state transitions in funds' currency-liquidity-timing behavior are driven by deteriorating external currency market liquidity conditions and negative shocks to internal fund returns.

Keywords: *Currency Factors, Endogenous Markov-Switching Models, Globally-Diversified Funds, Liquidity Timing.*

JEL Classification: *C32, F31, G11, G15, G23.*

*Email address: Luqi.Wang.2@bayes.city.ac.uk (Luqi Wang), G.Urga@city.ac.uk (Giovanni Urga). A previous version of the paper was presented at Bayes Business School, Banca Aletti, and the 25th Dynamic Econometrics Conference, and we wish to thank Siem Jan Koopman, Neil Ericsson, Richard Payne, Angelo Ranaldo, Chuanping Sun, Joshua Stillwagon, and Alessandro Varaldo for valuable comments. We are in debt with the Editor, Juan Francisco Rubio-Ramirez, and two anonymous referees for their useful comments and suggestions which helped improve the content and presentation of the paper. The usual disclaimer applies.

February 1, 2025

Optimal N-state endogenous Markov-switching model for currency liquidity timing

Abstract

In this paper, we examine whether globally-diversified funds' actively adjust their currency exposure in response to systematic currency liquidity movements, a behavior we term *currency liquidity timing*. A novel currency-liquidity-timing model embedded with an N-state endogenous Markov-switching mechanism is proposed to capture the dynamics in funds' timing behavior, as well as the external and internal drivers influencing such dynamics. Using a sample of 382 international fixed income mutual funds from July 2001 to December 2020, we find evidence of currency liquidity timing at the aggregate level for the sample funds. Interestingly, funds' currency-liquidity-timing behavior exhibits a state-switching pattern across different market periods: funds on average engage in perverse currency liquidity timing during tranquil market periods, but in positive currency liquidity timing with a stronger degree of aggressivity during more turbulent market periods. Our results suggest that the state transitions in funds' currency-liquidity-timing behavior are driven by deteriorating external currency market liquidity conditions and negative shocks to internal fund returns.

Keywords: *Currency Factors, Endogenous Markov-Switching Models, Globally-Diversified Funds, Liquidity Timing.*

JEL Classification: *C32, F31, G11, G15, G23.*

February 1, 2025

1. Introduction

The international asset pricing literature has firmly established that globally-diversified funds entail nontrivial exposure to the currency market (Brusa et al., 2014; Massa et al., 2016; Karolyi and Wu, 2021; Chaieb et al., 2021; Demirci et al., 2022). The recent study by Sialm and Zhu (2024) further reveals time variation in globally-diversified funds' currency exposure driven by their active adjustments. Along the line of this literature, an important subsequent question is what economic rationale underlies globally-diversified funds' active adjustments of their currency exposure. The first contribution of this paper is to examine empirically the validity of one potential explanation—these active adjustments may result from funds' responses to systematic (market-wide) currency liquidity movements, which we call *currency liquidity timing*. Such explanation is motivated by the fundamental role of systematic currency liquidity in determining market efficiency (Ranaldo and de Magistris, 2022) and trading frictions (e.g., price impacts, trading costs, and margin constraints) (Brunnermeier et al., 2008; Mancini et al., 2013; Filippou et al., 2024). Thus, systematic currency liquidity movements may be perceived by globally-diversified funds as signals of favorable (or adverse) changes in market efficiency and trading frictions related to the currency market. With the incentive to seek (or avoid) market-efficiency- and trading-friction-induced gains (or losses), funds may adjust their exposure either toward or away from the currency market,[1] ultimately resulting in active adjustments of their currency exposure.

To formalize the concept of currency liquidity timing, we build on the Cao et al. (2013b) model of liquidity timing, specifying fund currency exposure (which we call *currency beta*) as a function of demeaned systematic currency liquidity within the multifactor model of fund

[1]This can be achieved, for instance, by rebalancing the portfolio between foreign-currency-denominated and domestic-currency-denominated assets or by adjusting holdings of foreign currency derivatives (Sialm and Zhu, 2024).

return. We show that fund incentive to engage in a particular form of currency liquidity timing is reflected in the significance, sign and magnitude of the relation between currency beta and demeaned systematic currency liquidity, that is, the currency-liquidity-timing coefficient. Over time, globally-diversified funds may not engage in currency liquidity timing or otherwise in positive or perverse currency liquidity timing with varying degrees of aggressivity. This suggests the currency-liquidity-timing coefficient may manifest in multiple states, distinguishable by its significance, sign, or magnitude. Moreover, funds' timing decisions may be affected by external market conditions or internal fund performance. This suggests there might exist external or internal drivers affecting which state (and when) the currency-liquidity-timing coefficient may manifest in. The second contribution of this paper is therefore to propose a novel modeling framework for the currency-liquidity-timing coefficient with likely state switching. The proposed framework adopts an N-state endogenous Markov-switching model of Hwu et al. (2021), where the N states allow for the realization of multiple states in which the currency-liquidity-timing coefficient possibly manifests, and the endogenous Markov-switching mechanism flexibly accommodates external and internal drivers influencing the state transitions.

Methodologically, the proposed N-state endogenous Markov-switching model for currency liquidity timing is to some extent *optimal* compared with the existing return-based timing models.[2] First, our model estimates the timing coefficient across different states over the sample period, unlike conventional timing models with ordinary least squares (OLS) (see, e.g., Treynor and Mazuy, 1966; Cao et al., 2013b; Bali et al., 2021; Zheng et al., 2024, among many others) which estimate the timing coefficient for the entire sample period. Therefore, we take into account the potential dynamics in funds' timing behavior. Second, our model

[2]Holding-based timing models (see, e.g., Jiang et al., 2007; Elton et al., 2012) are beyond the scope of this paper.

enables the examination of multiple states with unknown switching dates underlying the timing coefficient, thereby encompassing a range of dynamic timing models that require either a priori known states or predetermined switching dates (see, e.g., Siegmann and Stefanova, 2017; Li et al., 2020a).[3] This, as shown in our empirical analysis (see Section 4.2), facilitates an extensive model estimation and comparison, ensuring that the states and switching dates inferred from the selected best-fitting model specification reflect the real data rather than being based on subjective beliefs. Third, our model investigates timing from a new perspective that focuses on the external and internal drivers influencing the state transitions in the timing coefficient. We show that external drivers can include certain indicators of external market conditions, while internal drivers are naturally represented by the error term in the proposed model (i.e., the idiosyncratic shocks to the modeled fund return series). In this way, we not only avoid biases in the timing coefficient estimate caused by ignoring endogeneity in state transitions (Hwu et al., 2021) but also explore the reasons driving funds' timing decision-making.

Our empirical analysis revisits the globally-diversified fund sample considered in Sialm and Zhu (2024), which includes 382 international fixed income mutual funds sourced from the CRSP Survivor-Bias-Free US Mutual Fund Database. In constructing the variables in the proposed model, we use the well-known currency factors proposed by Lustig et al. (2011)—the dollar factor and the carry-trade factor—to proxy the risk factors specific to the currency market; we use a set of four factors in Sialm and Zhu (2024)—the hedged global bond market factor, the emerging bond market factor, the term factor and the credit factor—to proxy additional risk factors that may influence the sample fund return; we exploit

[3]The changepoint timing model in Siegmann and Stefanova (2017) limits state switching to at most two dates, and the Markov-switching timing model in Li et al. (2020a) restricts state switching between two predefined states—the non-timing and timing states. Both are grounded on subjective beliefs, not reflecting the real data.

the widely used measure—the proportional quoted bid-ask spread—to proxy the systematic currency liquidity; we use a binary variable for relative liquidity conditions constructed in Li et al. (2020a) as a potential external driver of state transitions. With the constructed variables, the proposed model is estimated for an equally weighted monthly return series of sample funds during the sample period from July 2001 to December 2020. As such, the empirical usefulness of the proposed model is demonstrated by examining sample funds' currency-liquidity-timing behavior at the aggregate level.

The empirical results from the proposed model are summarized as follows. First, we find evidence of currency liquidity timing at the aggregate level for the sample funds. Interestingly, funds' currency-liquidity-timing behavior exhibits a state-switching pattern across different market periods: funds on average engage in perverse currency liquidity timing (i.e., adjust their currency exposure in a direction opposite to the systematic currency liquidity movements) during tranquil market periods, but in positive currency liquidity timing (i.e., adjust their currency exposure in a direction aligned with the systematic currency liquidity movements) with a stronger degree of aggressivity during more turbulent market periods. This is indicated by the best-fitting model specification with three distinct timing states: tranquil market periods are dominated by the model-implied *perverse timing* state where the currency-liquidity-timing coefficient estimates are negative; turbulent market periods are dominated by the model-implied *weakly positive timing* and *strongly positive timing* states where the currency-liquidity-timing coefficient estimates shift toward largely positive values. Motivated by the findings in Sialm and Zhu (2024), we associate the observed state-switching pattern of funds' currency-liquidity-timing behavior with their portfolio rebalancing and currency hedging practices. Second, we find the state transitions in funds' currency-liquidity-timing behavior appear to be driven by deteriorating external currency market liquidity conditions and negative shocks to internal fund returns. In particular, upon

worsening currency market liquidity conditions and poor performance, funds that previously engaged in perverse currency liquidity timing will be more likely to shift toward positive currency liquidity timing. This is suggested by the best-fitting model specification, in which both our constructed variable for relative liquidity conditions and the model's error term show minor negative effects on the probabilities of state transitions from the model-implied *perverse timing* state to the *weakly positive timing* and *strongly positive timing* states. Third, robustness checks reveal that while various controls appear to show some foreseeable impacts on the estimates in the best-fitting model specification, the aforementioned empirical results of currency liquidity timing are not explained away by funds' other behaviors, such as currency return timing, currency volatility timing and currency liquidity reaction.

The remainder of the paper is organized as follows. Section 2 sets up the model. Section 3 discusses the data and variables construction. Section 4 presents the empirical results. Section 5 conducts robustness checks. Section 6 concludes. Technical details and additional material on the robustness checks are provided in the Internet Appendix.

2. Model

Our model for currency liquidity timing is developed from the pioneering work of Cao et al. (2013b),[4] who show certain form of liquidity timing can be understood within the multifactor model of fund return. We exploit this insight from Cao et al. (2013b) to assume the following multifactor model generates a globally-diversified fund return

$$R_{p,t} = \alpha_p + \beta_{p,t}^{\text{Cur}} f_t^{\text{Cur}} + \sum_{j=1}^{J} \beta_p^j f_t^j + \varepsilon_{p,t}, \tag{1}$$

[4]Cao et al. (2013b) model of liquidity timing adheres to the traditional general models of return timing and volatility timing (see, e.g., Treynor and Mazuy, 1966; Ferson and Schadt, 1996; Busse, 1999), except that the market conditions considered is liquidity.

where p denotes a fund and t denotes a month; $R_{p,t}$ denotes the excess return of fund p (risk-free rate is proxied by the one-month Treasury bill rate); f_t^{Cur} denotes the risk factor specific to the currency market, with $\beta_{p,t}^{\text{Cur}}$ (hereafter *currency beta*) denoting the corresponding factor loading and capturing the currency exposure of fund p; $\{f_t^j\}_{j=1}^J$ denote the J additional risk factors, with $\{\beta_p^j\}_{j=1}^J$ denoting the corresponding factor loadings and capturing the additional risk exposures of fund p; α_p is the intercept, which captures the risk-adjusted abnormal return of fund p; $\varepsilon_{p,t}$, assumed to be independent and identically distributed as normal with a zero mean and variance σ^2 (i.e., $\varepsilon_{p,t} \sim$ i.i.d. $\mathcal{N}(0, \sigma^2)$), is the error term and captures the idiosyncratic shocks to return of fund p.

Let L_t^{Cur} denote systematic currency liquidity in month t, and $\bar{L}^{\text{Cur}}$ its historical average up to month t.[5] *Currency liquidity timing* refers to funds' active adjustments of currency exposure ($\beta_{p,t}^{\text{Cur}}$) in response to a timing signal measured as the difference between systematic currency liquidity (L_t^{Cur}) and its historical mean ($\bar{L}^{\text{Cur}}$), which according to Cao et al. (2013b) can be formulated as

$$\beta_{p,t}^{\text{Cur}} = \beta_p^{\text{Cur}} + \varphi_p(L_t^{\text{Cur}} - \bar{L}^{\text{Cur}}), \tag{2}$$

where β_p^{Cur} denotes the average currency beta of fund p without timing; φ_p denotes the currency-liquidity-timing coefficient of fund p. An insignificant φ_p indicates no currency liquidity timing: a fund maintains the currency exposure at the average level, that is $\beta_{p,t}^{\text{Cur}} = \beta_p^{\text{Cur}}$, regardless of systematic currency liquidity movements. A significant positive φ_p indicates *positive currency liquidity timing*: a fund increases (or reduces) currency exposure, that is $\beta_{p,t}^{\text{Cur}} > \beta_p^{\text{Cur}}$ (or $< \beta_p^{\text{Cur}}$), in response to upward (or downward) systematic currency liquidity movements. A significant negative φ_p indicates *perverse*[6] *currency liquidity timing*:

[5] We compute $\bar{L}^{\text{Cur}}$ using the time series mean of L_t^{Cur} over the previous 60 months as suggested by Cao et al. (2013b).

[6] Timing the market negatively is commonly referred to as *perverse* timing (see, e.g., Ferson and Schadt, 1996; Boney et al., 2009; Busse et al., 2024).

a fund reduces (or increases) currency exposure, that is $\beta_{p,t}^{\text{Cur}} < \beta_{p}^{\text{Cur}}$ (or $> \beta_{p}^{\text{Cur}}$), in response to upward (or downward) systematic currency liquidity movements. A large (or small) magnitude (i.e., absolute value) of φ_p indicates a fund strongly (or weakly) engages in positive or perverse currency liquidity timing.

In rationalizing why funds may be incentivized to engage in positive and perverse currency liquidity timing, previous literature suggests that systematic currency liquidity covaries positively with currency market performance due to its fundamental role in determining market efficiency (Ranaldo and de Magistris, 2022) and trading frictions (e.g., price impacts, trading costs, and margin constraints) (Brunnermeier et al., 2008; Mancini et al., 2013; Filippou et al., 2024). Positive currency liquidity timing therefore may occur when funds anticipate *persistence* in currency market performance (see, e.g., Menkhoff et al., 2012), adjusting their exposure toward (or away from) the currency market expected to perform better (or worse) alongside upward (or downward) liquidity movements. Perverse currency liquidity timing, on the other hand, may occur in two scenarios. First, funds might exploit liquidity-induced gains to reduce currency exposure (e.g., through currency hedging) when upward liquidity movements are perceived as indicating more mild trading frictions (e.g., lower hedging costs). Second, funds might anticipate *mean reversion* in currency market performance (see, e.g., Taylor, 2002; Serban, 2010), adjusting their exposure toward the currency market expected to revert in the long run even if it temporarily performs worse alongside downward liquidity movements.

Over time, funds may not engage in currency liquidity timing or otherwise in positive or perverse currency liquidity timing with varying degrees of aggressivity. This suggests the currency-liquidity-timing coefficient φ_p in (2) may manifest in multiple states, distinguishable by its significance, sign, or magnitude. Hence, we assume φ_p in month t manifests in one of N distinct states, which can be indicated by a latent Markov state variable s_t. Formally, we

express φ_p as a function of s_t as follows

$$\varphi_{p,s_t} = \sum_{n=1}^{N} \varphi_{p,n} \mathbb{I}(s_t = n), \tag{3}$$

where φ_{p,s_t} denotes the state-switching currency-liquidity-timing coefficient of fund p; $\varphi_{p,n}$ denotes the realization of φ_{p,s_t} in state n; $\mathbb{I}(\cdot)$ denotes the indicator function which takes value one if s_t indicates state n (i.e., s_t takes the value n from the set $\{1, ..., N\}$ in month t), and zero otherwise.

To specify further how the latent Markov state variable s_t indicates the N states over time, we assume the transition probabilities that s_t indicates state n in month $t-1$ and state j in month t for $n, j \in \{1, ..., N\}$, denoted by $p_{nj,t}$, is given by

$$p_{nj,t} = \Pr(s_t = j | s_{t-1} = n, z_t, \varepsilon_{p,t}), \tag{4}$$

where z_t (hereafter *transition covariates*) contains the variables expected to influence the state transitions; $\varepsilon_{p,t}$ is the error term in (1). (4) has several empirical implications and intuitions which we highlight as follows. First, the transition probabilities $p_{nj,t}$ are assumed to depend on transition covariates z_t, implying that z_t affects the realization of s_t and ultimately informs which state (and when) the currency-liquidity-timing coefficient manifests in (see (3)). Such an assumption is motivated by the existing evidence that state transitions in funds' liquidity-timing behavior tend to be driven by external market conditions. For example, Siegmann and Stefanova (2017) show that transitions in funds' stock-liquidity-timing behavior from the perverse timing state to the positive timing state are triggered by the market microstructure changes; Li et al. (2017) document that transitions in funds' bond-liquidity-timing behavior from the non-timing state to the timing state coincide with market crash. Thus, by choosing z_t as certain indicators of external market conditions,

(4) accommodates the external driver influencing the state transitions in funds' currency-liquidity-timing behavior. Second, the transition probabilities $p_{nj,t}$ are also assumed to depend on the error term $\varepsilon_{p,t}$, that is the idiosyncratic shocks to fund returns (see (1)). Such an assumption is motivated by the prior analyses of funds' active adjustments of risk exposure in relation to their performance. For example, Busse et al. (2023) suggest funds that trail in recent performance could be sensitive to their risk exposure in the hope of making up performance deficit or preventing themselves from falling further behind; Sialm and Zhu (2024) demonstrate that funds' active adjustments of currency exposure are sensitive to their downside returns. Thus, by viewing $\varepsilon_{p,t}$ as certain indicators of internal fund performance, (4) also accommodates the internal driver influencing the state transitions in funds' currency-liquidity-timing behavior.

To model the dependences of transition probabilities $p_{nj,t}$ on z_t and $\varepsilon_{p,t}$, we adopt an N-state endogenous Markov-switching model of Hwu et al. (2021), in which $s_t \in \{1, ..., N\}$ is alternatively described as the outcome of the values of $N-1$ mutually uncorrelated random variables, $s^*_{1,t}, s^*_{2,t}, ..., s^*_{N-1,t}$, such that

$$s_t = \begin{cases} 1 & \text{if } 0 = \max\left\{0, s^*_{1,t}, s^*_{2,t}, ..., s^*_{N-1,t}\right\} \\ 2 & \text{if } s^*_{1,t} = \max\left\{0, s^*_{1,t}, s^*_{2,t}, ..., s^*_{N-1,t}\right\} \\ \vdots & \\ N & \text{if } s^*_{N-1,t} = \max\left\{0, s^*_{1,t}, s^*_{2,t}, ..., s^*_{N-1,t}\right\} \end{cases} \tag{5}$$

where each of the $N-1$ random variables is assumed to follow the normal distribution

$$s^*_{i,t} \sim \mathcal{N}(\bar{\gamma}_{i,s_{t-1}} + z'_t \gamma^z_{i,s_{t-1}} + \rho_i \varepsilon_{p,t}, 1 - \rho_i^2), \tag{6}$$

for $i = 1, .., N-1$; $\bar{\gamma}_{i,s_{t-1}} = \sum_{n=1}^{N} \bar{\gamma}_{i,n} \mathbb{I}(s_{t-1} = n)$, $\gamma^z_{i,s_{t-1}} = \sum_{n=1}^{N} \gamma^z_{i,n} \mathbb{I}(s_{t-1} = n)$, and ρ_i

are parameters to be estimated (hereafter we collectively refer to as *transition parameters*). The transition parameters $\gamma^z_{i,s_{t-1}}$ and ρ_i allow the external and internal drivers to indirectly affect the realization of s_t through $s^*_{i,t}$. More specifically, with a significant positive $\gamma^z_{i,s_{t-1}}$, a higher value of transition covariate z_t leads to a higher value of $s^*_{i,t}$. Thus, $s^*_{i,t}$ is more likely to become the maximum among all the $N-1$ random variables, resulting in an increased probability that the s_t indicates state $(i+1)$ in month t (i.e., $s_t = i+1$ in (5)). Similarly, with a significant positive ρ_i, a larger positive idiosyncratic shock to fund return $\varepsilon_{p,t}$ leads to a higher value of $s^*_{i,t}$, resulting in an increased probability of $s_t = i+1$. It is also worth noting that the conventional class of exogenous Markov-switching models (see, e.g., Hamilton, 1989) is nested when transition parameters $\gamma^z_{i,s_{t-1}}$ and ρ_i are insignificant (i.e., in this case state transitions shown in (4) depend only on the realization of the previous state s_{t-1}).

Given (5)–(6), the transition probabilities $p_{nj,t}$ in (4) take the following form

$$\begin{aligned} p_{n1,t} &= \Pr(s_t = 1 | s_{t-1} = n, z_t, \varepsilon_{p,t}) \\ &= \Pr(s^*_{1,t} < 0, s^*_{2,t} < 0, ..., s^*_{N-1,t} < 0) \\ p_{nj,t} &= \Pr(s_t = j | s_{t-1} = n, z_t, \varepsilon_{p,t}) \\ &= \Pr(s^*_{j-1,t} > 0, \{s^*_{j-1,t} - s^*_{m,t} > 0 : m = 1, ..., N-1, m \neq j-1\}) \end{aligned} \tag{7}$$

for $n \in \{1, ..., N\}$ and $j \in \{2, ..., N\}$ (See the Internet Appendix A for the detailed derivation).

The final form of our proposed N-state endogenous Markov-switching model for currency liquidity timing can be summarized as

$$R_{p,t} = \alpha_p + \beta^{\text{Cur}}_p f^{\text{Cur}}_t + \varphi_{p,s_t}(L^{\text{Cur}}_t - \bar{L}^{\text{Cur}}) f^{\text{Cur}}_t + \sum_{j=1}^{J} \beta^j_p f^j_t + \varepsilon_{p,t}, \tag{8}$$

which is derived by replacing φ_p in (2) with φ_{p,s_t} in (3) and then substituting (2) into (1);

where $s_t \in \{1, ..., N\}$ and the associated state transitions are formulated by (5)–(7).

3. Data and variables construction

To conduct an empirical analysis, we revisit the globally-diversified fund sample considered in Sialm and Zhu (2024), which includes international fixed income mutual funds sourced from the CRSP Survivor-Bias-Free US Mutual Fund Database. Specifically, we select funds whose stated objectives indicate that they specialize in international fixed income investments, and exclude passively-managed index funds and ETFs from the fund sample.[7] The dataset on international fixed income mutual funds expands Sialm and Zhu (2024) as it spans from July 2001 to December 2020 at the monthly frequency. Individual fund-level return is the average across its share classes returns using share classes' total net assets (TNA) in the previous month as the weight.[8] Individual fund-level TNA is the sum of TNAs among its share classes. Following the convention in fund timing studies (see, e.g., Siegmann and Stefanova, 2017; Bali et al., 2021), we further restrict our sample to funds that have at least two years of returns and a minimum of $10 million in TNA.[9] The final sample consists of

[7]We select funds whose CRSP objective code (as identified by *crsp_obj_cd*) is IF, which cover six Lipper objectives: Emerging Markets Debt Funds (EMD), Emerging Markets Local Currency Funds (EML), Global High Yield Funds (GHY), Global Income Funds (GLI), International Income Funds (INI), and Short World Multi-Market Income Funds (SWM). Among these funds, we exclude funds whose CRSP identifiers "*index_fund_flag*" indicates a B, D or E or "*et_flag*" indicates an ETF or ETN. According to the CRSP Survivor-Bias-Free US Mutual Fund Guide (https://www.crsp.org/research/crsp-survivor-bias-free-us-mutual-funds/), EMD funds seek either current income or total return by investing primarily in emerging market debt securities, where emerging market is defined by a country's GNP per capita or other economic measures. EML funds seek either current income or total return by investing at least 65% of total assets in emerging market debt issues denominated in the currency of their market of issuance. GHY funds aim at high (relative) currency yield from both domestic and foreign fixed income securities, have no quality or maturity restrictions, and tend to invest in lower-grade debt issues. GLI funds invest primarily in US dollar and non-US dollar debt securities of issuers located in at least three countries, one of which may be the United States. INI funds invest primarily in non-US dollar and US dollar debt securities of issuers located in at least three countries, excluding the US, except in periods of market weakness. SWM funds invest in non-US dollar and US dollar debt instruments and, by policy, keep a dollar-weighted average maturity of less than five years.

[8]The share class's missing TNA is imputed as with Ibert et al. (2018).

[9]We include a fund as soon as its inflation-adjusted TNA reached $10 million. Our inflation index is the Consumer Price Index for All Urban Consumers (CPIAUCSL) series provided by the Federal Reserve Bank of St. Louis' FRED database. The data are available from https://fred.stlouisfed.org/series/CPIAUCSL.

382 international fixed income mutual funds. All individual fund-level returns in the sample are then equally weighted[10] to construct $R_{p,t}$ in (8), which provides a natural examination of sample funds' timing behavior at the aggregate level.[11]

Following the international asset pricing literature (Brusa et al., 2014; Massa et al., 2016; Karolyi and Wu, 2021; Chaieb et al., 2021; Demirci et al., 2022), we construct f_t^{Cur} in (8) by the well-known currency factors proposed by Lustig et al. (2011)—the dollar factor (RX) and the carry-trade factor (HML_FX). Intuitively, RX is the return on an equally weighted portfolio of long positions in major non-US dollar currencies, while HML_FX is the return on a zero-cost strategy that goes long high-interest rate currencies and goes short low-interest rate currencies. Thus the former mimics the currency market return available to the globally-diversified fund with US dollar as their base currency, while the latter captures global risk for which the globally-diversified fund earns a carry-trade risk premium. Both factors are obtained from the authors' website.[12]

As in Sialm and Zhu (2024), we construct $\{f_t^j\}_{j=1}^J$ in (8) by the following four factors (J=4 in this case): the hedged global bond market factor (GMF), the emerging bond market factor (EMF), the term factor (TERM), and the credit factor (CREDIT). The data for the hedged global bond market factor, the emerging bond market factor, and the credit factor are obtained from Bloomberg. The hedged global bond market factor is proxied by the return

[10]Here we do not consider the TNA (value) weighted return because the individual fund-level TNA is unavailable for some funds in some months. Excluding these fund samples or imputing the missing fund-month TNA observations could introduce biases in the resulting weighted return, which explains why many fund timing studies rely on the equally weighted return for aggregate-level timing analyses (see, e.g., Boney et al., 2009; Chen et al., 2010; Zheng et al., 2024). Besides, several studies considering both weighting strategies show that the timing results derived from the equally weighted and value weighted returns are qualitatively similar (see, e.g., Chen and Liang, 2007; Cao et al., 2013b).

[11]Given the detailed implementation of model estimation and comparison (see Section 4.2), this paper demonstrates the empirical usefulness of the proposed model primarily through an analysis at the aggregate level for all sample funds. This analysis is insightful for understanding general trends in sample funds' average timing behavior and the underlying state-switching pattern. Nevertheless, the proposed model is adaptable to analyses at a more granular level, such as fund subgroups (e.g., categorized by fund performance or characteristics) or an individual fund of interest. We leave these analyses as directions for future investigation.

[12]See http://web.mit.edu/adrienv/www/Data.html.

of the Bloomberg Global Aggregate Bond Index USD hedged. The emerging bond market factor is proxied by the return of the JPMorgan Emerging Market Bond Index Global. The credit factor is the difference between the returns of the Bloomberg US Aggregate BAA Index and the Bloomberg US Aggregate AAA Index. The data for the term factor is obtained from the Board of Governors of the Federal Reserve System. The term factor is defined as the difference between the ten-year Treasury return minus the one-month Treasury return.

Consistent with the expanding literature on systematic currency liquidity (see, e.g., Kessler and Scherer, 2011; Menkhoff et al., 2012; Karnaukh et al., 2015; Li et al., 2020b), we construct L_t^{Cur} in (8) by the widely used measure—the proportional quoted bid-ask spread.[13] Formally,

$$L_t^{\text{Cur}} = \frac{1}{T_t}\sum_{\tau=1}^{T_t}\Big(\frac{1}{I}\sum_{i=1}^{I} -\frac{P_{i,\tau}^A - P_{i,\tau}^B}{P_{i,\tau}^M}\Big), \tag{9}$$

where t denotes a month and τ denotes a day; T_t denotes the total number of trading days in month t; $\{P_{i,\tau}^A\}_{i=1}^I$, $\{P_{i,\tau}^B\}_{i=1}^I$, and $\{P_{i,\tau}^M\}_{i=1}^I = \{0.5(P_{i,\tau}^A + P_{i,\tau}^B)\}_{i=1}^I$ denote respectively the quoted ask price, bid price, and their midpoint for currency i (all against the US dollar) in a basket of I currencies on day τ.[14] The daily $\{P_{i,\tau}^A\}_{i=1}^I$ and $\{P_{i,\tau}^B\}_{i=1}^I$ for all the currencies are obtained from Thomson Reuters' Datastream. The monthly L_t^{Cur}, as shown in (9), is calculated by first averaging all currencies' daily negative bid-ask spreads and then averaging these daily values up to the monthly frequency. Thus, the lower L_t^{Cur}, the more illiquid the currency market. In addition, since currency spreads are small in magnitude, we further

[13] Although there are several other measures for systematic currency liquidity (e.g., those based on price impact, return reversal, effective costs and price dispersion), evidence shows the proportional quoted bid-ask spread is highly correlated with these measures. For instance, the correlation documented in Mancini et al. (2013) is 0.853 for the proportional quoted bid-ask spread and price impact, 0.890 for return reversal, 0.954 for effective costs, and 0.949 for price dispersion.

[14] For consistency, we consider a basket in Lustig et al. (2011), which covers currencies from the following regions: Australia, Canada, Hong Kong, euro area, India, Indonesia, Japan, Kuwait, Malaysia, Mexico, New Zealand, Norway, Philippines, Saudi Arabia, Singapore, South Africa, South Korea, Switzerland, Taiwan, Thailand, and the United Kingdom. Since the currency of euro area was introduced in January 1999 (which covers our sample period), the currencies of euro area countries, originally considered in Lustig et al. (2011), are excluded and only the currency of euro area is retained.

rescale L_t^{Cur} by multiplying 1000 to facilitate interpretability of the coefficient estimates in the empirical analyses in Sections 4–5. Figure 1 plots the time path of the systematic currency liquidity L_t^{Cur}. We observe a strong upward trend at the beginning of the sample period, which is primarily driven by the introduction of electronic trading systems that substantially increase liquidity (Li et al., 2020b). We also observe several downward spikes line up with known liquidity events affecting the currency market, for example, the sub-prime and the European sovereign debt crises between 2008–2009 and the COVID-19 crisis in early 2020. Therefore, the constructed systematic currency liquidity L_t^{Cur} seems to capture obvious times of currency market distress quite well.

In the spirit of Li et al. (2020a) who point out the nonnegligible effect of different market liquidity conditions on changes in funds' liquidity-timing behavior, we construct z_t in (5)–(7) as a binary variable taking the value one or zero based on whether the current systematic currency liquidity L_t^{Cur} above/below its historical average $\bar{L}^{\text{Cur}}$

$$z_t = \begin{cases} 1 & \text{if } L_t^{\text{Cur}} > \bar{L}^{\text{Cur}} \\ 0 & \text{otherwise} \end{cases} \tag{10}$$

such that z_t represents the currency market relative liquidity conditions in month t.

Table 1 presents descriptive statistics. Panel A reports the statistics of sample fund characteristics. The reported age is the number of years between fund's last performance date and fund's first offer date, where fund's last performance date is taken to be the latest net asset values (NAV) date across its share classes while fund's first offer date is taken to be the earliest first offer date across its share classes. The reported TNA is the total net asset in million US dollar, the reported expense is the annual expense ratio in percentage, the reported turnover is the annual turnover ratio in percentage, and the reported return is the monthly return in percentage. Except for the reported age which is averaged across

all sample funds, other reported characteristics are first averaged over time for each fund, and then averaged across all sample funds. Panel A shows that, on average, an international fixed income mutual fund in the sample has TNA of $708 million, an annual expense ratio of 0.82%, an age of around 13 years, an annual turnover ratio of 112.34%, and a monthly return of 0.372%. Panel B reports the statistics of risk factors (monthly in percentage) and systematic currency liquidity (monthly in bps). For instance, the average dollar factor (RX) during the sample period is 0.185% per month with a standard deviation of 1.775%.

4. Empirical results

Given the variables constructed in Section 3, the empirical form of our proposed model (8) is given by[15]

$$\begin{aligned} R_t = &\alpha + \beta^{\text{HML\_FX}}\text{HML\_FX}_t + \mu_{s_t}(L_t^{\text{Cur}} - \bar{L}^{\text{Cur}})\text{HML\_FX}_t + \beta^{\text{RX}}\text{RX}_t + \lambda_{s_t}(L_t^{\text{Cur}} - \bar{L}^{\text{Cur}})\text{RX}_t \\ &+ \beta^{\text{GMF}}\text{GMF}_t + \beta^{\text{EMF}}\text{EMF}_t + \beta^{\text{TERM}}\text{TERM}_t + \beta^{\text{CREDIT}}\text{CREDIT}_t + \varepsilon_t, \end{aligned} \tag{11}$$

where t denotes a month; $s_t \in \{1, ..., N\}$ and the associated state transitions are formulated by (5)–(7); R_t is the equally weighted return of all sample funds; HML_FX_t and RX_t are the risk factors specific to the currency market—the carry-trade and the dollar factors; GMF_t, EMF_t, TERM_t and CREDIT_t are the additional risk factors—the hedged global bond market factor, the emerging bond market factor, the term factor, and the credit factor; L_t^{Cur} is the systematic currency liquidity and $\bar{L}^{\text{Cur}}$ its historical average; μ_{s_t} and λ_{s_t} are currency-liquidity-timing coefficients of interest.

[15] In (11), we drop the subscript p (that denotes a fund) from (8) for notational convenience.

4.1. Preliminary analysis: currency liquidity timing without state switching

We begin our analysis of currency liquidity timing without state switching. We follow conventional timing models (see, e.g., Treynor and Mazuy, 1966; Cao et al., 2013b; Bali et al., 2021; Zheng et al., 2024, among many others) to implement OLS on the non-state-switching variant of (11), where μ_{s_t} and λ_{s_t} are replaced with constant values μ and λ. The results are in Table 2, showing that μ is negative and statistically significant at the 5% level while λ is insignificant. Therefore, the main takeaway from this preliminary analysis is that sample funds engage in currency liquidity timing—especially in a perverse way—only when adjusting their currency exposure with respect to the carry-trade factor.

However, it is worth noting that the non-state-switching variant of (11) implicitly assumes that sample funds engage in either currency liquidity timing or not over the entire sample period, and thus what the OLS really estimates is funds' currency-liquidity-timing behavior averaged over the entire sample period under investigation. Consequently, when funds engage in currency liquidity timing strategically and intermittently, rather than continuously over the sample period of study, the evidence of the potential currency-liquidity-timing behavior during certain time periods may be averaged out, impacting upon the significance of the currency-liquidity-timing coefficient estimates. In this aspect, even if OLS implies a statistically insignificant λ, we can not rule out the possibility that funds may engage in currency liquidity timing when adjusting their currency exposure with respect to the dollar factor during a certain time period. We now explore this possibility using the original state-switching form of (11) in the next subsection.

4.2. Model estimation and comparison: currency liquidity timing with state switching

We undertake an extensive model estimation and comparison to select the best-fitting state-switching model specification from the variants of (11). These variants are labeled as $\mathcal{M}_{R,N}$ in that they differ along two dimensions—the state-switching restrictions R and the

number of states N. Specifically, we first consider three different state-switching restrictions ($R = 1, 2, 3$), leading to the following model specifications based on (11): (i) $R = 1$ (denoted by $\mathcal{M}_{1,N}$): μ_{s_t} is replaced with a constant value μ, (ii) $R = 2$ (denoted by $\mathcal{M}_{2,N}$): λ_{s_t} is replaced with a constant value λ, and (iii) $R = 3$ (denoted by $\mathcal{M}_{3,N}$): the original form of (11). As such, $\mathcal{M}_{1,N}$ and $\mathcal{M}_{2,N}$ allow only one currency-liquidity-timing coefficient to be state-switching while the other to remain constant; $\mathcal{M}_{3,N}$ allows both to be state-switching and thus is the model specification with the most stringent state-switching restriction. We then consider three different numbers of states ($N = 2, 3, 4$). Overall, we have in total nine state-switching model specifications $\mathcal{M}_{1,2}$, $\mathcal{M}_{1,3}$, $\mathcal{M}_{1,4}$, $\mathcal{M}_{2,2}$, $\mathcal{M}_{2,3}$, $\mathcal{M}_{2,4}$, $\mathcal{M}_{3,2}$, $\mathcal{M}_{3,3}$, and $\mathcal{M}_{3,4}$.

To estimate a given state-switching model specification, we adopt a simulation-based Bayesian inference procedure of Kim and Kang (2022) (see the Internet Appendix B for details), which offers computational advantages over Hwu et al. (2021)'s maximum-likelihood inference procedure when estimating the class of N-state endogenous Markov-switching models with larger values of N. For state identification and interpretation purposes, we impose the inequality constraints on the currency-liquidity-timing coefficients through the Bayesian inference procedure.[16] Particularly, for model specifications $\mathcal{M}_{1,N}$ and $\mathcal{M}_{2,N}$ with $N = 2, 3, 4$, we impose respectively $\lambda_{s_t=1} < \lambda_{s_t=2} < ... < \lambda_{s_t=N}$ and $\mu_{s_t=1} < \mu_{s_t=2} < ... < \mu_{s_t=N}$; for model specification $\mathcal{M}_{3,N}$ with $N = 2, 3, 4$, we impose jointly $\lambda_{s_t=1} < \lambda_{s_t=2} < ... < \lambda_{s_t=N}$ and $\mu_{s_t=1} < \mu_{s_t=2} < ... < \mu_{s_t=N}$.[17]

[16] Inequality constraints are imposed via rejection sampling, as with Kim and Kang (2022).

[17] For $\mathcal{M}_{3,N}$ with $N = 2, 3, 4$, it would be possible to impose the inequality constraints on λ_{s_t} and μ_{s_t} separately rather than jointly. We therefore examine whether imposing the inequality constraints jointly is too stringent. In the case of $N = 3$, we note the log marginal likelihoods (computed as in the Internet Appendix B) of $\mathcal{M}_{3,3}$ with a constraint on λ_{s_t} or μ_{s_t} alone are 904.301 and 895.508, respectively. These values are substantially smaller than that of $\mathcal{M}_{3,3}$ with constraints on λ_{s_t} and μ_{s_t} jointly, which is 920.402. Similar results are observed in the cases of $N = 2$ and $N = 4$. Thus, imposing the inequality constraints jointly for $\mathcal{M}_{3,N}$ seems to be appropriate.

To evaluate the in-sample fit of each estimated state-switching model specification, we use the marginal likelihood—a natural output from the simulation-based Bayesian inference procedure (see the Internet Appendix B for details). To formally compare the model specifications' marginal likelihoods, we use the pairwise log-Bayes factor, the ratio (in logarithm) of the marginal likelihood of one reference model specification to the marginal likelihood of each alternative model specification. With this definition, the log-Bayes factor of the reference model specification versus itself equals zero. Kass and Raftery (1995) suggest interpreting the log-Bayes factor between 0 and 0.5 as weak evidence in favor of the reference model specification, between 1 and 2 as strong evidence, and greater than 2 as decisive evidence. The negative log-Bayes factor of the same magnitude is said to favor the alternative model specification by the same amount (Jiang et al., 2013). Table 3 presents the pairwise log-Bayes factors in favor of the reference model specification $\mathcal{M}_{1,2}$[18] over itself and the other eight state-switching model specifications considered. By looking at the log-Bayes factors column-by-column, model specifications are compared in terms of the state-switching restrictions $R = 1, 2, 3$. In the case of $N = 2$, the log-Bayes factor of 4.0 indicates that $\mathcal{M}_{2,2}$ is less preferred compared to $\mathcal{M}_{1,2}$. By contrast, the log-Bayes factor of -3.9 provides substantial evidence in favor of model $\mathcal{M}_{3,2}$ against $\mathcal{M}_{1,2}$. Similar patterns are observed for $N = 3, 4$. Thus, it is clear that log-Bayes factors tend to favor the model specification with $R = 3$ where both currency-liquidity-timing coefficients are state-switching. By looking at the log-Bayes factors row-by-row, model specifications are compared in terms of the number of states $N = 2, 3, 4$. We observe that $\mathcal{M}_{1,3}$, $\mathcal{M}_{2,3}$ and $\mathcal{M}_{3,3}$ achieve the lowest log-Bayes factor in their respective columns, meaning that $N = 3$ (i.e., three states) overwhelms the other number of states. Combining these findings, $\mathcal{M}_{3,3}$ (i.e., the original form of (11) with

[18] Alternative choices of the reference model specification do not change the conclusions from our log-Bayes factor comparison.

three states $s_t \in \{1, 2, 3\}$) yields the lowest log-Bayes factor of -8.1 and thus is the best-fitting state-switching model specification among all the nine variants of (11).

Table 4 presents the posterior summary of the best-fitting state-switching model specification $\mathcal{M}_{3,3}$, which includes the posterior means, standard errors, 95% highest posterior density interval (HPDI)[19] and convergence statistics (inefficiency factor and Geweke (1992)'s p-value as in Kim and Kang (2022)) of the model parameters' posterior samples. The inefficiency factors, when compared to those in Kim and Kang (2022), are generally in a similar range to indicate low autocorrelation of model parameters' posterior samples. The Geweke (1992)'s p-values are all greater than 0.05, which are good signs of convergence of model parameters' posterior samples (LeSage, 1999). Overall, these results indicate the well-mixing and convergence properties of parameters' posterior samples obtained from the best-fitting state-switching model specification $\mathcal{M}_{3,3}$.

4.3. Model-implied states of currency liquidity timing

Panel B of Table 4 presents the posterior summary of the currency-liquidity-timing coefficients μ_{s_t} and λ_{s_t} specific to the model-implied three states $s_t \in \{1, 2, 3\}$. We find evidence of currency liquidity timing for the sample funds across all three states, given that both coefficients' corresponding 95% HPDIs are never centered on zero. Particularly, according to the interpretation in (2), the model-implied state $s_t = 1$ is the state where sample funds engage in perverse currency liquidity timing (hereafter *perverse timing* state), given that the posterior means of μ_1 and λ_1 are negative and their corresponding 95% HPDIs completely fall below zero. The model-implied state $s_t = 2$ is the state where sample funds engage in positive currency liquidity timing with a relatively weak degree of aggressivity (hereafter

[19]The 95% highest posterior density interval (HPDI) contains 95% mass of the parameter's posterior distribution. Reporting the HPDI to indicate the statistical significance of the estimated parameters is a common practice in the empirical Bayesian literature (see, e.g., Giaccotto et al., 2011; Chalamandaris, 2020; Ulm and Hambuckers, 2022).

weakly positive timing state), given that the posterior means of μ_2 and λ_2 are positive and their corresponding 95% HPDIs mostly fall above zero. The model-implied state $s_t = 3$ is the state where sample funds engage in positive currency liquidity timing with a relatively strong degree of aggressivity (hereafter *strongly positive timing* state), given that the posterior means of μ_3 and λ_3 are positive and their corresponding 95% HPDIs completely fall above zero.

Panel D of Table 4 presents the posterior summary of the state differences in currency-liquidity-timing coefficients $\mu_2 - \mu_1$, $\mu_3 - \mu_2$, $\lambda_2 - \lambda_1$,$\lambda_3 - \lambda_2$. We observe that all reported 95% HPDIs exclude zero, thereby confirming statistically that there are three distinct timing states characterized by statistically different currency-liquidity-timing coefficients $\mu_{s_t=1,2,3}$ and $\lambda_{s_t=1,2,3}$.

Figure 5 plots the shaded areas[20] that highlight the periods of sample funds being in a particular model-implied state. We find tranquil market periods are dominated by the *perverse timing* state, while turbulent market periods are dominated by the *weakly positive timing* and *strongly positive timing* states. The periods under the *weakly positive timing* state are July 2001-August 2001, December 2002-May 2003, September 2004-December 2004, July 2011-February 2012, August 2013-January 2014, December 2014-May 2015, August 2015-December 2015, August 2018-December 2018, and May 2020-July 2020, covering the early 2000s recession, several rounds of US Quantitative Easing (QE) programs from 2009 to 2015, and the COVID-19 crisis in early 2020. The period under the *strongly positive timing* state is May 2009-December 2009, covering the aftermath of the sub-prime crisis; for example, the credit crisis with Greece's Bailout taking place after 2009.

[20]The shaded areas highlight the periods during which the probability of each model-implied state is greater than a threshold of 50%. Given the M posterior samples of s_t, the probability of each state in month t can be easily approximated by $\frac{1}{M}\sum_{m=1}^{M}\mathbb{I}(s_t = n)$, for $n = 1, 2, 3$. A threshold of 50% is extensively used in empirical studies with Markov-switching models (see. e.g., Chan et al., 2011; Jutasompakorn et al., 2014).

Taken together, the above findings suggest that sample funds' currency-liquidity-timing behavior exhibits a state-switching pattern across different market periods: they engage in perverse currency liquidity timing during tranquil market periods, but engage in positive currency liquidity timing with a stronger degree of aggressivity during more turbulent market periods. In conjecturing the mechanism that interprets such state-switching pattern, we are motivated by prior research of Sialm and Zhu (2024) indicating that portfolio rebalancing and currency hedging are chief mechanisms through which sample funds actively adjust their currency exposure. For instance, sample funds can switch from domestic-currency-denominated to foreign-currency-denominated assets (i.e., more foreign holdings) or shrink the short positions in foreign currency derivatives (i.e., less currency hedging) to increase their currency exposure.

During tranquil market periods when currency exchange rate fluctuations are relatively stable, funds possibly do not engage in frequent portfolio rebalancing because doing so is costly (Opie and Riddiough, 2020) and the adverse depreciation of foreign currencies is relatively short-lived. As a result, changes in funds' currency exposure may mainly result from currency hedging. When receiving upward (or downward) liquidity signals, funds perceive these as indicators of low (or high) hedging costs to hedge more (or less), leading to a reduction (or an increase) in their currency exposure. This causes funds' currency betas to shift in a direction opposite to the systematic currency liquidity movements, resulting in the observed *preserve currency liquidity timing*.

During turbulent market periods when currency exchange rate fluctuations are relatively volatile, funds possibly engage in frequent portfolio rebalancing because the adverse depreciation of foreign currencies is relatively persistent (which makes the potential loss from re-denominating returns on foreign-currency-denominated assets to the domestic currency unbearable). Funds tend to exhibit a stronger *home-currency bias*—reducing currency expo-

sure whenever possible (Burger et al., 2018; Maggiori et al., 2020). This drives them to switch back to domestic-currency-denominated assets (i.e., less foreign holdings). In such situations, both portfolio rebalancing and currency hedging come into play. When systematic currency liquidity moves downward further, funds become more risk-averse to switch more intensively back to domestic-currency-denominated assets and hedge more aggressively, leading to a further reduction in their currency exposure. Consequently, funds' currency betas shift in a direction more aligned with the systematic currency liquidity's downward movements, resulting in the observed *weakly positive currency liquidity timing* and *strongly positive currency liquidity timing*.

4.4. Model-implied drivers of currency liquidity timing

Panel C of Table 4 presents the posterior summary of $\gamma^z_{1,s_{t-1}}$ and $\gamma^z_{2,s_{t-1}}$ specific to the model-implied three states $s_{t-1} = 1, 2, 3$. From (6)–(7), these parameters reflect the effects of the currency market relative liquidity conditions z_t (defined in (10)) on the transition probabilities of different timing states. Generally, we observe that the posterior means of $\{\gamma^z_{1,s_{t-1}=n}\}^3_{n=1}$ and $\{\gamma^z_{2,s_{t-1}=n}\}^3_{n=1}$ are negative and their corresponding 95% HPDIs mostly fall below zero. As further confirmed in Figure 2, though the distributions of $\{\gamma^z_{1,s_{t-1}=n}\}^3_{n=1}$ and $\{\gamma^z_{2,s_{t-1}=n}\}^3_{n=1}$ are assumed to be centered on zero a priori, their posterior distributions appear to shift toward the negative region. These results, taken as a whole, indicate the minor negative effects of the currency market relative liquidity conditions z_t on state transitions in sample funds' currency-liquidity-timing behavior.

To explain in more detail, we compute the transition probabilities $p_{nj,t} = \Pr(s_t = j | s_{t-1} = n, z_t)$ for the model-implied three states (i.e., $n, j \in \{1, ..., 3\}$), which are variants of (7) conditional on the information from z_t alone (See the Internet Appendix A for the detailed derivation). For the scenario where the currency market is relatively liquid (i.e., $z_t = 1$ in (10)), the matrix that collects the transition probabilities $p_{nj,t} = \Pr(s_t = j | s_{t-1} = n, z_t = 1)$,

denoted by $P_t(z_t = 1)$, is

$$P_t(z_t = 1) = \begin{pmatrix} p_{11,t} & p_{12,t} & p_{13,t} \\ p_{21,t} & p_{22,t} & p_{23,t} \\ p_{31,t} & p_{32,t} & p_{33,t} \end{pmatrix} = \begin{pmatrix} 0.892 & 0.094 & 0.014 \\ 0.192 & 0.719 & 0.088 \\ 0.096 & 0.143 & 0.761 \end{pmatrix}. \tag{12}$$

For the scenario where the currency market is relatively illiquid (i.e., $z_t = 0$ in (10), the matrix that collects the transition probabilities $p_{nj,t} = \Pr(s_t = j | s_{t-1} = n, z_t = 0)$, denoted by $P_t(z_t = 0)$, is

$$P_t(z_t = 0) = \begin{pmatrix} p_{11,t} & p_{12,t} & p_{13,t} \\ p_{21,t} & p_{22,t} & p_{23,t} \\ p_{31,t} & p_{32,t} & p_{33,t} \end{pmatrix} = \begin{pmatrix} 0.890 & 0.089 & 0.022 \\ 0.092 & 0.828 & 0.080 \\ 0.054 & 0.139 & 0.807 \end{pmatrix}. \tag{13}$$

We first look at the self-transition probabilities $\{p_{nn,t}\}_{n=1}^{3}$ in (12)–(13). We observe that a decreasing z_t increases greatly $p_{22,t}$ and $p_{33,t}$ while nearly not affecting $p_{11,t}$. Thus among the model-implied three states, the *weakly positive timing* and *strongly positive timing* states are more sensitive to the worsening currency market liquidity conditions than the *perverse timing* state. Specifically, if samples funds previously were in the *weakly positive timing* or *strongly positive timing* states (i.e., $s_{t-1} = 2$ or 3), they will be more likely to continuously stay in the same states (i.e., $s_t = 2$ or 3) under the worsening currency market liquidity conditions. As such, falling systematic currency liquidity makes the *weakly positive timing* or *strongly positive timing* states last longer. We then turn to the remaining non-self-transition probabilities in (12)–(13). First, we can see a decreasing z_t slightly reduces $p_{12,t}$ but increases $p_{13,t}$. This indicates if samples funds previously were in the *perverse timing* state (i.e., $s_{t-1} = 1$), they will be more likely to switch to the *strongly positive timing* state (i.e., $s_t = 3$) than to the *weakly positive timing* state (i.e., $s_t = 2$) under the worsening

currency market liquidity conditions. Second, we can see a decreasing z_t slightly reduces $p_{21,t}$, $p_{23,t}$, $p_{31,t}$ and $p_{32,t}$. This, as suggested by the self-transition probabilities $p_{22,t}$ and $p_{33,t}$, is not surprising since worsening currency market liquidity conditions make sample funds more likely to continuously stay in the *weakly positive timing* or *strongly positive timing* states, which in turn means they are less likely to switch to other states.

Overall, the lower z_t (i.e., the worsening currency market liquidity conditions) is somewhat associated with the realization of higher s_t (i.e., the *weakly positive timing* and *strongly positive timing* states). This explains the observed minor negative effects of z_t on state transitions in sample funds' currency-liquidity-timing behavior. Such finding is consistent with the observations in Figure 5 that turbulent market periods, known to be accompanied with the currency market illiquidity, are dominated by the *weakly positive timing* and *strongly positive timing* states.

Panel C of Table 4 also presents the posterior summary of ρ_1 and ρ_2. From (6)–(7), these parameters reflect the effects of the idiosyncratic shocks to fund returns ε_t (defined in (1)) on the transition probabilities of different timing states. Generally, we observe that the posterior mean of ρ_1 is negative, while that of ρ_2 is almost zero. As further confirmed in Figure 3, though the distributions of ρ_1 and ρ_2 are assumed to be centered on zero a priori, the posterior distribution of ρ_1 appears to shift toward the negative region while that of ρ_2 appears to be around zero. These results, taken as a whole, indicate the negative effects of the idiosyncratic shocks to fund returns ε_t on state transitions in sample funds' currency-liquidity-timing behavior to the *weakly positive timing* state, while negligible effects on state transitions to the *strongly positive timing* state.

To explain in more detail, we compute the transition probabilities $p_{nj,t} = \Pr(s_t = j | s_{t-1} = n, \varepsilon_t)$ for the model-implied three states (i.e., $n, j \in \{1, ..., 3\}$), which are variants of (7)

conditional on the information from ε_t alone.[21] The transition probabilities $p_{nj,t} = \Pr(s_t = j|s_{t-1} = n, \varepsilon_t)$ against artificial realizations of $\varepsilon_t \in [-10, 10]$ are plot in Figure 4. We first look at the self-transition probabilities $\{p_{nn,t}\}_{n=1}^{3}$. We observe that a decreasing ε_t increases $p_{22,t}$ but reduces $p_{11,t}$ and $p_{33,t}$. Thus among the model-implied three states, the *weakly positive timing* state is more sensitive to funds' poor performance than the *perverse timing* and *strongly positive timing* states. Specifically, if sample funds previously were in the *weakly positive timing* state (i.e., $s_{t-1} = 2$), they will be more likely to continuously stay in the same state (i.e., $s_t = 2$) given funds' poor performance. We then turn to the remaining non-self-transition probabilities. First, we can see a decreasing ε_t increases greatly $p_{12,t}$ and $p_{32,t}$ while nearly not affecting $p_{13,t}$ and $p_{31,t}$. This indicates if sample funds previously were in the *perverse timing* or *strongly positive timing* states (i.e., $s_{t-1} = 1$ or 3), they will be more likely to switch to the *weakly positive timing* state (i.e., $s_t = 2$) than to other states given funds' poor performance. Second, we can see a decreasing ε_t reduces $p_{21,t}$ and $p_{23,t}$. This, as suggested by the self-transition probabilities $p_{22,t}$, is not surprising since funds' poor performance makes sample funds more likely to continuously stay in the *weakly positive timing* state, which in turn means they are less likely to switch to other states.

Overall, the lower ε_t (i.e., funds' poor performance) is somewhat associated with the realization of $s_t = 2$ (i.e., the *weakly positive timing* state). This explains why the estimated ρ_1 is sizable and displays a negative sign. Such finding points out two scenarios: sample funds, given poor performance, are incentivized to (i) switch from the *perverse timing* state to the *weakly positive timing* state or (ii) switch from the *strongly positive timing* state to the *weakly positive timing* state. We conjecture that the first scenario occurs when sample funds experience poor performance at the onset of market deterioration. In this scenario, funds that previously paid little attention to their currency exposure may become more

[21] This can be computed by imposing zero values on transition parameters $\gamma^z_{1,s_{t-1}}$ and $\gamma^z_{2,s_{t-1}}$ in (6)–(7).

concerned as they face increased outflows due to poor performance and worsening market conditions (Chen, Q. et al., 2010). As a result, funds are likely to switch from leaving their currency exposure unhedged (i.e., the *perverse timing* state) to possibly hedging their currency exposure (i.e., the *weakly positive timing*) when systematic currency liquidity begins to move downward. We conjecture that the second scenario occurs when sample funds experience poor performance at the onset of market recovery. In this scenario, funds that previously were highly concerned about their currency exposure may begin to calm down. While still mindful of liquidity-induced losses due to poor performance, funds may develop certain risk appetites. As a result, funds are likely to change the degree of aggressivity of their currency-liquidity-timing behavior, switching from aggressive timing (i.e., the *strongly positive timing* state) to more moderate timing (i.e., the *weakly positive timing* state).

5. Robustness checks

This section conducts robustness checks, which further test the aforementioned empirical results obtained from the best-fitting state-switching model specification $\mathcal{M}_{3,3}$ (see Section 4.2). We discuss results in the following subsections and present supporting tables and figures in the Internet Appendix C.

5.1. Controlling for currency return and volatility timing

Funds may engage in timing in various ways, such as return timing and volatility timing (see, e.g., Chen and Liang, 2007; Bodson et al., 2013). Much of the studies suggest that systematic (market-wide) currency liquidity is positively correlated with systematic currency return and negatively correlated with systematic currency volatility (see, e.g., Melvin and Taylor, 2009; Menkhoff et al., 2012; Mancini et al., 2013). Thus, it would be possible that the evidence on currency liquidity timing can be partially attributed to funds' currency-

return-timing or currency-volatility-timing behaviors. To address this concern, we control for currency return and volatility timing in the model specification $\mathcal{M}_{3,3}$.

Table C.1 in the Internet Appendix C presents the posterior summary of the model specification $\mathcal{M}_{3,3}$ with controls for currency return and volatility timing. From Panel B, we observe the evidence of perverse currency liquidity timing becomes relatively weaker in the model-implied state $s_t = 1$, as the 95% HPDIs of μ_1 and λ_1 mostly, but not completely, fall below zero. This is consistent with Cao et al. (2013a) who document that controlling for market-return and volatility timing reduces the significance of perverse liquidity timing. Despite that, there is virtually no difference between most results in Table C.1 and those in Table 4. As shown in Figure C.1 (a) in the Internet Appendix C, the periods of sample funds being in a particular model-implied state are highly comparable to those depicted in Figure 5. Overall, though the evidence of perverse currency liquidity timing is not as strong as previously observed, both currency return and volatility timing do not severely affect the state-switching behavior of currency liquidity timing among the sample funds.

5.2. Currency liquidity timing versus currency liquidity reaction

Cao et al. (2013a) argue that funds may also adjust their factor exposure based on lagged values of liquidity. If funds use observed liquidity in time $t-1$ to derive a predictable component of liquidity and adjust their factor beta accordingly, they do not engage in timing but simply react to public information (Ferson and Schadt, 1996). Given this conjecture, it would be possible that the evidence on currency liquidity timing might rather reflect funds' responses to lagged systematic currency liquidity. To distinguish currency liquidity timing from currency liquidity reaction, we follow Cao et al. (2013a) and extend the model specification $\mathcal{M}_{3,3}$ to include both liquidity timing and liquidity reaction terms.

Table C.2 in the Internet Appendix C presents the posterior summary of the model specification $\mathcal{M}_{3,3}$ with controls for currency liquidity reaction. From Panel A, we observe

significant evidence of currency liquidity reaction as the 95% HPDIs of the liquidity-reaction coefficients $\psi^{\text{HML\_FX}}$ and ψ^{RX} completely fall below zero and above zero, respectively. The results in Panels B–C of Table C.2 are again highly similar to those in Table 4, though the effects of the idiosyncratic shocks to fund returns ε_t on state transitions in sample funds' currency-liquidity-timing behavior are marginal in this case. As shown in Figure C.1 (b) in the Internet Appendix C, the *weakly positive timing* and *strongly positive timing* states occur less frequently than those depicted in Figure 5, implying that some periods of positive currency liquidity timing are partly results of funds' responses to previous systematic currency liquidity. Overall, there is a certain level of currency liquidity reaction among sample funds, but funds' state-switching currency-liquidity-timing behavior cannot be fully attributed to liquidity reaction.

5.3. Discussions

We draw several conclusions from the robustness checks. First, various controls appear to show some foreseeable impacts on the model-implied three states and the endogenous state transitions. Specifically, we observe the weakening evidence of the three distinct states in various robustness checks. Moreover, we observe the diminishing evidence that idiosyncratic shocks to fund returns ε_t affect state transitions in sample funds' currency-liquidity-timing behavior when controls are in place. These observations are expected in robustness checks because a number of extra controls which are added to the model specification $\mathcal{M}_{3,3}$ tend to capture part of the explanatory power of the variables already included. Thus, it is natural to anticipate a reduction in the significance of currency-liquidity-timing coefficients[22] as well as the significance of transition parameters associated with the error term.

[22]Similar observations have been reported, for instance, by Chen et al. (2010) where the timing coefficients which are significantly negative in the original model are found to appear neutral to weakly positive when augmenting the model with several controls for nonlinearity.

Second, the empirical results previously obtained from the model specification $\mathcal{M}_{3,3}$ in Section 4 remain largely unchanged under all the robustness checks: (i) the evidence on currency liquidity timing among sample funds is not explained away by funds' other behaviors, such as currency return timing, currency volatility timing and currency liquidity reaction. This is supported by the observations that both currency-liquidity-timing coefficients' corresponding 95% HPDIs are never centered on zero; (ii) the state-switching pattern that funds' currency-liquidity-timing behavior switches from the *perverse timing* state toward the *weakly positive timing* and *strongly positive timing* states remains robust under different controls. This is evidenced by the observations that for both timing coefficients, their 95% HPDIs which cover a larger negative region in the model-implied state $s_t = 1$ appear to move toward the positive region in the model-implied states $s_t = 2, 3$; (iii) systematic currency liquidity continues to show minor negative effects on state transitions in sample funds' currency-liquidity-timing behavior. This is reflected by the overall negative estimates of $\gamma^z_{1,s_{t-1}}$ and $\gamma^z_{2,s_{t-1}}$.

6. Conclusions

In this paper, we examined if globally-diversified funds' active adjustments of currency exposure may result from their responses to systematic currency liquidity movements, which we call *currency liquidity timing*. A novel currency-liquidity-timing model embedded with an N-state endogenous Markov-switching mechanism was proposed to capture the potential dynamics in funds' timing behavior, as well as the external and internal drivers influencing such dynamics. Using a sample of 382 international fixed income mutual funds from July 2001 to December 2020 as a testing ground, the empirical usefulness of the proposed model was demonstrated by examining sample funds' currency-liquidity-timing behavior at the aggregate level. The empirical results showed evidence of currency liquidity timing at the

aggregate level for the sample funds. Interestingly, funds' currency-liquidity-timing behavior was found to exhibit a state-switching pattern across different market periods: funds on average engage in perverse currency liquidity timing (i.e., adjust their currency exposure in a direction opposite to the systematic currency liquidity movements) during tranquil market periods, but in positive currency liquidity timing (i.e., adjust their currency exposure in a direction aligned with the systematic currency liquidity movements) with a stronger degree of aggressivity during more turbulent market periods. We explained that this state-switching pattern is possibly attributed to funds' portfolio rebalancing and currency hedging practices. The model also indicated that the state transitions in funds' currency-liquidity-timing behavior appear to be driven by deteriorating external currency market liquidity conditions and negative shocks to internal fund returns. Under the robustness checks, while various controls appeared to show some foreseeable impacts on the model estimates, the aforementioned empirical results of currency liquidity timing were not explained away by funds' other behaviors, such as currency return timing, currency volatility timing, currency liquidity reaction, and holding illiquid assets.

References

Bali, T.G., Brown, S.J., Caglayan, M.O., Celiker, U., 2021. Does industry timing ability of hedge funds predict their future performance, survival, and fund flows? Journal of Financial and Quantitative Analysis 56, 2136–2169.

Bodson, L., Cavenaile, L., Sougné, D., 2013. A global approach to mutual funds market timing ability. Journal of Empirical Finance 20, 96–101.

Boney, V., Comer, G., Kelly, L., 2009. Timing the investment grade securities market: Evidence from high quality bond funds. Journal of Empirical Finance 16, 55–69.

Brunnermeier, M.K., Nagel, S., Pedersen, L.H., 2008. Carry trades and currency crashes. NBER Macroeconomics Annual 23, 313–348.

Brusa, F., Ramadorai, T., Verdelhan, A., 2014. The international CAPM redux. Saïd Business School Working Paper. Available at: https://core.ac.uk/download/pdf/288287858.pdf.

Burger, J.D., Warnock, F.E., Warnock, V.C., 2018. Currency matters: Analyzing international bond portfolios. Journal of International Economics 114, 376–388.

Busse, J.A., 1999. Volatility timing in mutual funds: Evidence from daily returns. The Review of Financial Studies 12, 1009–1041.

Busse, J.A., Ding, J., Jiang, L., Tang, Y., 2023. Artificial market timing in mutual funds. Journal of Financial and Quantitative Analysis 58, 3450–3481.

Busse, J.A., Ding, J., Jiang, L., Wu, K., 2024. Dynamic market timing in mutual funds. Management Science 70, 3470–3492.

Cao, C., Chen, Y., Liang, B., Lo, A.W., 2013a. Can hedge funds time market liquidity? Journal of Financial Economics 109, 493–516.

Cao, C., Simin, T.T., Wang, Y., 2013b. Do mutual fund managers time market liquidity? Journal of Financial Markets 16, 279–307.

Chaieb, I., Langlois, H., Scaillet, O., 2021. Factors and risk premia in individual international stock returns. Journal of Financial Economics 141, 669–692.

Chalamandaris, G., 2020. Assessing the relevance of an information source to trading from an adaptive-markets hypothesis perspective. Quantitative Finance 20, 1101–1122.

Chan, K.F., Treepongkaruna, S., Brooks, R., Gray, S., 2011. Asset market linkages: Evidence from financial, commodity and real estate assets. Journal of Banking & Finance 35, 1415–1426.

Chen, Y., Ferson, W., Peters, H., 2010. Measuring the timing ability and performance of bond mutual funds. Journal of Financial Economics 98, 72–89.

Chen, Y., Liang, B., 2007. Do market timing hedge funds time the market? Journal of Financial and Quantitative Analysis 42, 827–856.

Chen, Q., Goldstein, I., Jiang, W., 2010. Payoff complementarities and financial fragility: Evidence from mutual fund outflows. Journal of Financial Economics 97, 239–262.

Demirci, I., Ferreira, M.A., Matos, P., Sialm, C., 2022. How global is your mutual fund? International diversification from multinationals. The Review of Financial Studies 35, 3337–3372.

Elton, E.J., Gruber, M.J., Blake, C.R., 2012. An examination of mutual fund timing ability using monthly holdings data. Review of Finance 16, 619–645.

Ferson, W.E., Schadt, R.W., 1996. Measuring fund strategy and performance in changing economic conditions. The Journal of Finance 51, 425–461.

Filippou, I., Maurer, T.A., Pezzo, L., Taylor, M.P., 2024. Importance of transaction costs for asset allocation in foreign exchange markets. Journal of Financial Economics 159, 103886.

Geweke, J., 1992. Evaluating the accuracy of sampling-based approaches to the calculations of posterior moments. Bayesian Statistics 4, 641–649.

Giaccotto, C., Golec, J., Vernon, J., 2011. New estimates of the cost of capital for pharmaceutical firms. Journal of Corporate Finance 17, 526–540.

Hamilton, J.D., 1989. A new approach to the economic analysis of nonstationary time series and the business cycle. Econometrica 57, 357–384.

Hwu, S.T., Kim, C.J., Piger, J., 2021. An N-state endogenous Markov-switching model with applications in macroeconomics and finance. Macroeconomic Dynamics 25, 1937–1965.

Ibert, M., Kaniel, R., Van Nieuwerburgh, S., Vestman, R., 2018. Are mutual fund managers paid for investment skill? The Review of Financial Studies 31, 715–772.

Jiang, G.J., Yao, T., Yu, T., 2007. Do mutual funds time the market? Evidence from portfolio holdings. Journal of Financial Economics 86, 724–758.

Jiang, X., Yuan, Y., Mahadevan, S., Liu, X., 2013. An investigation of Bayesian inference approach to model validation with non-normal data. Journal of Statistical Computation and Simulation 83, 1829–1851.

Jutasompakorn, P., Brooks, R., Brown, C., Treepongkaruna, S., 2014. Banking crises: Identifying dates and determinants. Journal of International Financial Markets, Institutions and Money 32, 150–166.

Karnaukh, N., Ranaldo, A., Söderlind, P., 2015. Understanding FX liquidity. The Review of Financial Studies 28, 3073–3108.

Karolyi, G.A., Wu, Y., 2021. Is currency risk priced in global equity markets? Review of Finance 25, 863–902.

Kass, R.E., Raftery, A.E., 1995. Bayes factors. Journal of the American Statistical Association 90, 773–795.

Kessler, S., Scherer, B., 2011. Hedge fund return sensitivity to global liquidity. Journal of Financial Markets 14, 301–322.

Kim, Y.M., Kang, K.H., 2022. Bayesian inference of multivariate regression models with endogenous Markov regime-switching parameters. Journal of Financial Econometrics 20, 391–436.

LeSage, J.P., 1999. Applied econometrics using MATLAB, Manuscript, Dept. of Economics, University of Toledo.

Li, B., Luo, J., Tee, K.H., 2017. The market liquidity timing skills of debt-oriented hedge funds. European Financial Management 23, 32–54.

Li, C., Li, B., Tee, K.H., 2020a. Are hedge funds active market liquidity timers? International Review of Financial Analysis 67, 101415.

Li, C., Li, B., Tee, K.H., 2020b. Measuring liquidity commonality in financial markets. Quantitative Finance 20, 1553–1566.

Lustig, H., Roussanov, N., Verdelhan, A., 2011. Common risk factors in currency markets. The Review of Financial Studies 24, 3731–3777.

Maggiori, M., Neiman, B., Schreger, J., 2020. International currencies and capital allocation. Journal of Political Economy 128, 2019–2066.

Mancini, L., Ranaldo, A., Wrampelmeyer, J., 2013. Liquidity in the foreign exchange market: Measurement, commonality, and risk premiums. The Journal of Finance 68, 1805–1841.

Massa, M., Wang, Y., Zhang, H., 2016. Benchmarking and currency risk. Journal of Financial and Quantitative Analysis 51, 629–654.

Melvin, M., Taylor, M.P., 2009. The crisis in the foreign exchange market. Journal of International Money and Finance 28, 1317–1330.

Menkhoff, L., Sarno, L., Schmeling, M., Schrimpf, A., 2012. Carry trades and global foreign exchange volatility. The Journal of Finance 67, 681–718.

Opie, W., Riddiough, S.J., 2020. Global currency hedging with common risk factors. Journal of Financial Economics 136, 780–805.

Ranaldo, A., de Magistris, P.S., 2022. Liquidity in the global currency market. Journal of Financial Economics 146, 859–883.

Serban, A.F., 2010. Combining mean reversion and momentum trading strategies in foreign exchange markets. Journal of Banking & Finance 34, 2720–2727.

Sialm, C., Zhu, Q., 2024. Currency management by international fixed-income mutual funds. The Journal of Finance 79, 4037–4081.

Siegmann, A., Stefanova, D., 2017. The evolving beta-liquidity relationship of hedge funds. Journal of Empirical Finance 44, 286–303.

Taylor, A.M., 2002. A century of purchasing-power parity. Review of Economics and Statistics 84, 139–150.

Treynor, J., Mazuy, K., 1966. Can mutual funds outguess the market. Harvard Business Review 44, 131–136.

Ulm, M., Hambuckers, J., 2022. Do interest rate differentials drive the volatility of exchange rates? Evidence from an extended stochastic volatility model. Journal of Empirical Finance 65, 125–148.

Zheng, Y., Osmer, E., Zu, D., 2024. Timing sentiment with style: Evidence from mutual funds. Journal of Banking & Finance 164, 107197.

Table 1: Descriptive statistics

	Mean	Std. Dev.	P25	P50	P75
Panel A: Fund characteristics					
TNA ($ mil.)	708	1,392	46	202	630
Expense (%)	0.82	0.33	0.63	0.83	1.03
Age (years)	13.3	8.8	6.5	10.4	18.1
Turnover (%)	112.34	114.71	52.18	78.91	124.12
Return (%)	0.372	0.248	0.238	0.381	0.497
Panel B: Risk factors and systematic currency liquidity					
GMF (%)	0.277	0.798	-0.285	0.328	0.834
EMF (%)	0.575	2.581	-0.390	0.788	1.865
TERM (%)	0.153	0.091	0.082	0.163	0.221
CREDIT (%)	0.193	1.646	-0.385	0.267	0.778
HML_FX (%)	0.434	2.247	-0.823	0.501	1.888
RX (%)	0.185	1.775	-0.830	0.239	1.237
L_t^{Cur} (bps)	-6.862	1.808	-7.709	-6.594	-5.302

NOTES: This table presents descriptive statistics, including the means (Mean), standard deviations (Std. Dev.), 25th percentiles (P25), medians (P50), and 75th percentiles (P75). Panel A reports these statistics of sample fund characteristics, including the total net asset in million US dollar (TNA), annual expense ratio in percentage (Expense), age in years (Age), annual turnover ratio in percentage (Turnover), and monthly return in percentage (Return). Except for the reported age which is averaged across all sample funds, other reported characteristics are first averaged over time for each fund, and then averaged across all sample funds. Panel B reports these statistics of monthly systematic currency liquidity in bps (L_t^{Cur}) and monthly risk factors in percentage, including the hedged global bond market factor (GMF), the emerging bond market factor (EMF), the term factor (TERM), the credit factor (CREDIT), the carry-trade factor (HML_FX) and the dollar factor (RX). The fund sample consists of 382 international fixed income mutual funds sourced from the CRSP Survivor-Bias-Free US Mutual Fund Database. The sample period spans from July 2001 to December 2020.

Table 2: Estimation results of the non-state-switching model specification

α (%)	β^{GMF}	β^{EMF}	β^{TERM}	β^{CREDIT}	$\beta^{\text{HML\_FX}}$	β^{RX}	μ	λ	Adj R^2
-0.05	0.38***	0.24***	0.34	0.29***	0.01	0.43***	-0.10**	-0.05	0.97
(-1.13)	(11.91)	(14.99)	(1.42)	(13.73)	(1.10)	(27.59)	(-2.19)	(-0.95)	

NOTES: This table presents the estimation results of the non-state-switching variant of (11). The model specification is given by

$$\begin{aligned} R_t = &\alpha + \beta^{\text{HML\_FX}}\text{HML\_FX}_t + \mu(L_t^{\text{Cur}} - \bar{L}^{\text{Cur}})\text{HML\_FX}_t + \beta^{\text{RX}}\text{RX}_t + \lambda(L_t^{\text{Cur}} - \bar{L}^{\text{Cur}})\text{RX}_t \\ &+ \beta^{\text{GMF}}\text{GMF}_t + \beta^{\text{EMF}}\text{EMF}_t + \beta^{\text{TERM}}\text{TERM}_t + \beta^{\text{CREDIT}}\text{CREDIT}_t + \varepsilon_t, \end{aligned}$$

where t denotes a month; R_t is the equally weighted return of all sample funds; HML_FX_t and RX_t are the risk factors specific to the currency market—the carry-trade and the dollar factors; GMF_t, EMF_t, TERM_t and CREDIT_t are the additional risk factors—the hedged global bond market factor, the emerging bond market factor, the term factor, and the credit factor; L_t^{Cur} is the systematic currency liquidity and $\bar{L}^{\text{Cur}}$ its historical average; μ and λ are currency-liquidity-timing coefficients of interest. Results are based on ordinary least squares (OLS). The t-statistics are reported in parentheses. The adjusted R-square (Adj R^2) is reported in the last column. ***, ** denote significance at 1% and 5% levels, respectively. The sample period spans from July 2001 to December 2020.

Table 3: Pairwise log-Bayes factors of the state-switching model specifications $\mathcal{M}_{R,N}$

	$R = 1$	$R = 2$	$R = 3$
$N = 2$	0.0	4.0	-3.9
$N = 3$	-2.6	3.0	-8.1
$N = 4$	-1.7	4.6	-7.0

NOTES: This table presents the pairwise log-Bayes factors of the state-switching model specifications $\mathcal{M}_{R,N}$ developed from the variants of (11), for three different state-switching restrictions $R = 1, 2, 3$ and number of states $N = 2, 3, 4$. The value reported in each cell is the log-Bayes factor in favor of the reference model specification $\mathcal{M}_{1,2}$ over the alternative model specification $\mathcal{M}_{R,N}$ with R and N labeled as the cell's column and row. The log-Bayes factor of the reference model specification versus itself equals zero. Kass and Raftery (1995) suggest interpreting the log-Bayes factor between 0 and 0.5 as weak evidence in favor of the reference model specification, between 1 and 2 as strong evidence, and greater than 2 as decisive evidence. The negative log-Bayes factor of the same magnitude is said to favor the alternative model specification by the same amount (Jiang et al., 2013).

Table 4: Estimation results of the selected state-switching model specification $\mathcal{M}_{3,3}$

	s_t/s_{t-1}	Mean	s.e.	95% HPDI		Ineff	p-val
Panel A: Non-state-switching coefficients							
α (%)		0.083	0.011	[0.082,	0.124]	68.900	0.816
β^{GMF}		0.054	0.009	[0.052,	0.091]	68.467	0.718
β^{EMF}		0.065	0.003	[0.065,	0.074]	61.332	0.922
β^{TERM}		1.479	0.071	[1.195,	1.496]	70.630	0.691
β^{CREDIT}		0.108	0.009	[0.105,	0.144]	69.826	0.679
$\beta^{\text{HML\_FX}}$		-0.001	0.005	[-0.019,	0.000]	68.773	0.783
β^{RX}		0.179	0.007	[0.150,	0.180]	71.379	0.717
σ		0.004	0.000	[0.004,	0.005]	1.932	0.296
Panel B: Currency-liquidity-timing coefficients							
μ_{s_t}	1	-0.076	0.018	[-0.136,	-0.072]	69.515	0.672
	2	0.086	0.038	[-0.032,	0.096]	71.740	0.669
	3	0.633	0.117	[0.283,	0.663]	71.959	0.674
λ_{s_t}	1	-0.813	0.091	[-0.836,	-0.544]	69.586	0.677
	2	0.874	0.246	[-0.072,	0.939]	73.790	0.658
	3	1.767	0.269	[0.834,	1.838]	72.721	0.662
Panel C: Transition parameters							
$\bar{\gamma}_{1,s_{t-1}}$	1	-1.342	0.198	[-1.719,	-0.938]	6.355	0.730
	2	1.150	0.199	[0.770,	1.550]	5.190	0.693
	3	-0.136	0.208	[-0.535,	0.278]	1.203	0.942
$\gamma^z_{1,s_{t-1}}$	1	0.026	0.255	[-0.487,	0.514]	2.453	0.846
	2	-0.445	0.271	[-0.951,	0.104]	5.983	0.693
	3	-0.179	0.295	[-0.759,	0.395]	1.439	0.896
$\bar{\gamma}_{2,s_{t-1}}$	1	-2.001	0.220	[-2.430,	-1.575]	3.508	0.533
	2	-0.645	0.200	[-1.035,	-0.252]	2.209	0.677
	3	1.295	0.211	[0.895,	1.718]	2.218	0.650
$\gamma^z_{2,s_{t-1}}$	1	-0.167	0.278	[-0.694,	0.394]	2.409	0.733
	2	-0.199	0.278	[-0.766,	0.330]	1.653	0.842
	3	-0.277	0.281	[-0.824,	0.264]	1.450	0.758
ρ_1		-0.431	0.251	[-0.780,	0.218]	52.937	0.676
ρ_2		0.009	0.208	[-0.390,	0.428]	14.468	0.624
Panel D: State differences in currency-liquidity-timing coefficients							
$\mu_2 - \mu_1$		0.163	0.021	[0.104,	0.168]	70.000	0.683
$\mu_3 - \mu_2$		0.547	0.080	[0.315,	0.567]	71.530	0.678
$\lambda_2 - \lambda_1$		1.687	0.332	[0.472,	1.775]	73.535	0.658
$\lambda_3 - \lambda_2$		0.893	0.052	[0.899,	0.906]	57.614	0.869

NOTES: This table presents the posterior summary of the best-fitting state-switching model specification $\mathcal{M}_{3,3}$, including the posterior means (Mean), the posterior standard errors (s.e.), 95% highest posterior density interval (95% HPDI), inefficiency factor (Ineff) and Geweke (1992)'s p-value (p-val) of the obtained parameters' posterior samples. The model specification is given by

$$\begin{aligned} R_t = &\alpha + \beta^{\text{HML\_FX}}\text{HML\_FX}_t + \mu_{s_t}(L_t^{\text{Cur}} - \bar{L}^{\text{Cur}})\text{HML\_FX}_t + \beta^{\text{RX}}\text{RX}_t + \lambda_{s_t}(L_t^{\text{Cur}} - \bar{L}^{\text{Cur}})\text{RX}_t \\ &+ \beta^{\text{GMF}}\text{GMF}_t + \beta^{\text{EMF}}\text{EMF}_t + \beta^{\text{TERM}}\text{TERM}_t + \beta^{\text{CREDIT}}\text{CREDIT}_t + \varepsilon_t, \end{aligned}$$

where t denotes a month; $s_t \in \{1, 2, 3\}$ and the associated state transitions are formulated by (5)–(7); R_t is the equally weighted return of all sample funds; HML_FX_t and RX_t are the risk factors specific to the currency market—the carry-trade and the dollar factors; GMF_t, EMF_t, TERM_t and CREDIT_t are the additional risk factors—the hedged global bond market factor, the emerging bond market factor, the term factor, and the credit factor; L_t^{Cur} is the systematic currency liquidity and $\bar{L}^{\text{Cur}}$ its historical average; μ_{s_t} and λ_{s_t} are currency-liquidity-timing coefficients of interest. Results are based on a simulation-based Bayesian inference procedure with 12,500 iterations. The sample period spans from July 2001 to December 2020.

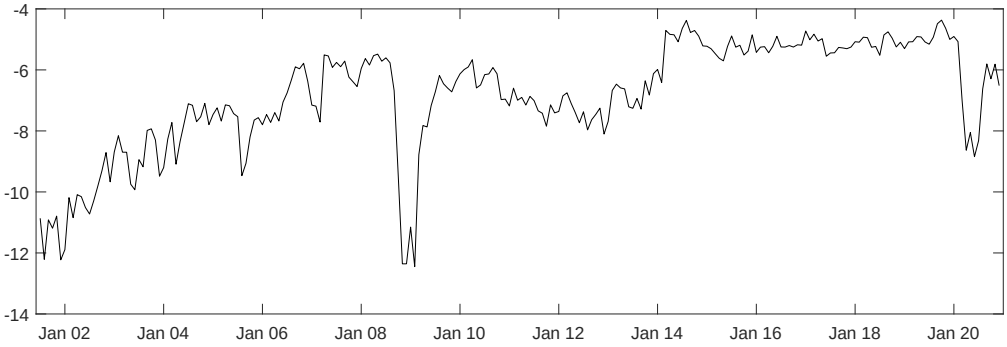

Figure 1: Time path of the systematic currency liquidity L_t^{Cur}. This figure plots systematic currency liquidity L_t^{Cur} over time, calculated by first averaging all sample currencies' daily negative bid-ask spreads and then averaging these daily values up to the monthly frequency. Thus, the lower L_t^{Cur}, the more illiquid the currency market. The sample currencies include 21 currencies considered in Lustig et al. (2011) against the US dollar. The sample period spans from July 2001 to December 2020.

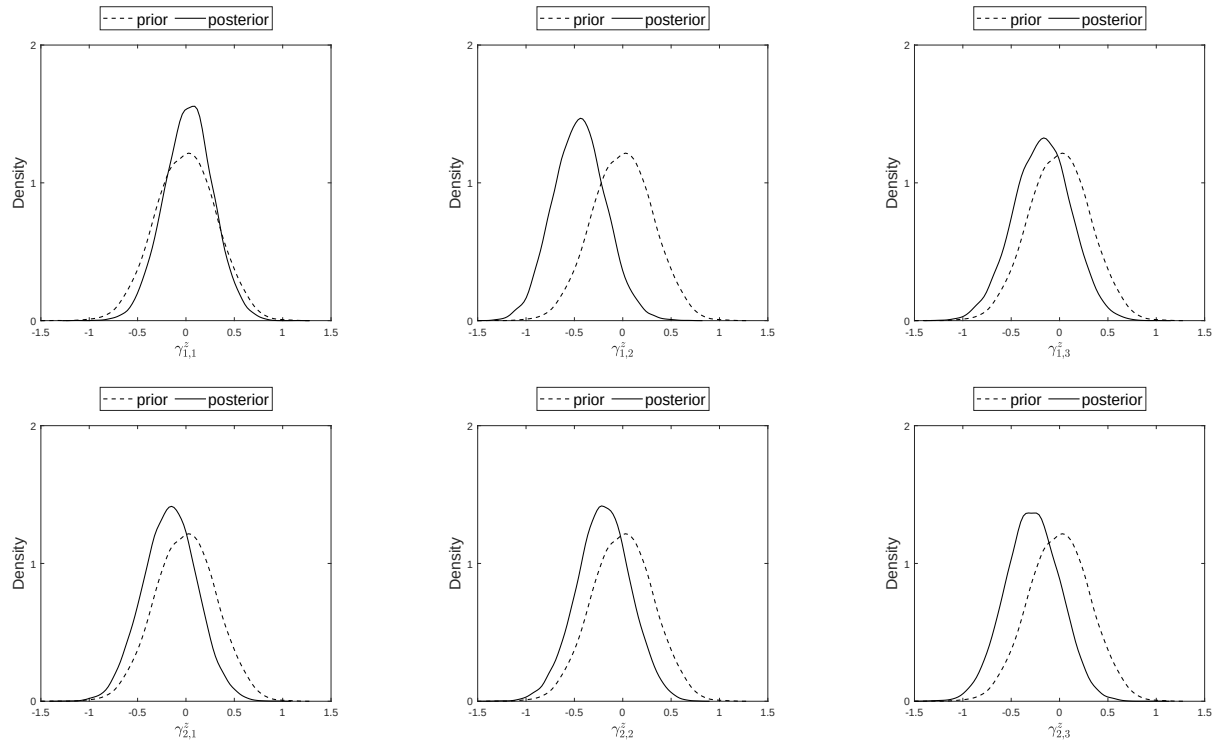

Figure 2: Prior-posterior distributions of the transition parameters $\{\gamma^z_{1,s_{t-1}=n}\}^3_{n=1}$ and $\{\gamma^z_{2,s_{t-1}=n}\}^3_{n=1}$ obtained from the best-fitting state-switching model specification $\mathcal{M}_{3,3}$. Each plot displays the posterior distribution (solid line) against the prior distribution (dashed line) of a given transition parameter. Results are based on a simulation-based Bayesian inference procedure with 12,500 iterations.

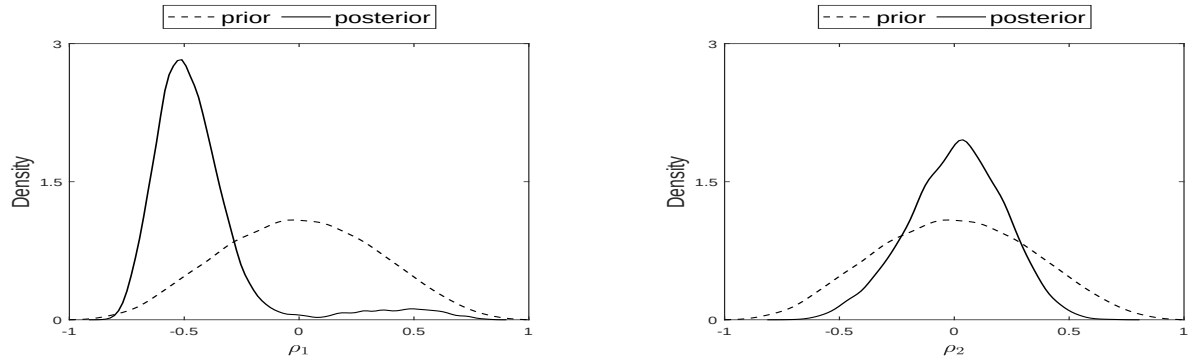

Figure 3: Prior-posterior distributions of the transition parameters ρ_1 and ρ_2 obtained from the best-fitting state-switching model specification $\mathcal{M}_{3,3}$. Each plot displays the posterior distribution (solid line) against the prior distribution (dashed line) of a given transition parameter. Results are based on a simulation-based Bayesian inference procedure with 12,500 iterations.

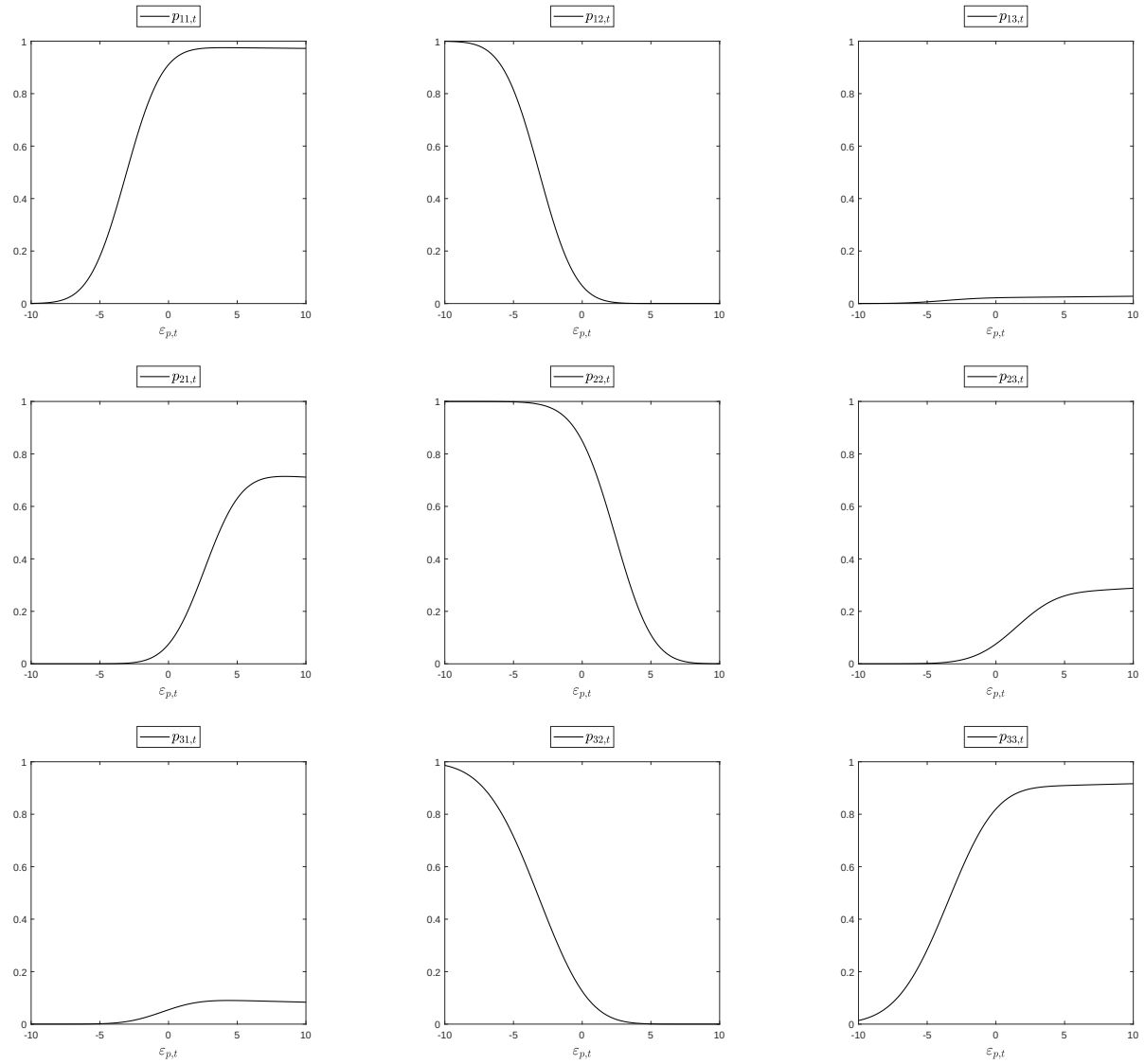

Figure 4: Transition probabilities $p_{nj,t} = \Pr(s_t = j | s_{t-1} = n, \varepsilon_t)$, $n, j \in \{1, ..., 3\}$, against artificial realizations of $\varepsilon_t \in [-10, 10]$ computed from the best-fitting state-switching model specification $\mathcal{M}_{3,3}$. Each plot displays a given transition probability (solid line) conditional on the information from the error term ε_t alone. The x-axis measures alternative values of $\varepsilon_t \in [-10, 10]$. The y-axis measures alternative values of transition probabilities $p_{nj,t} \in [0, 1]$. Results are based on a simulation-based Bayesian inference procedure with 12,500 iterations.

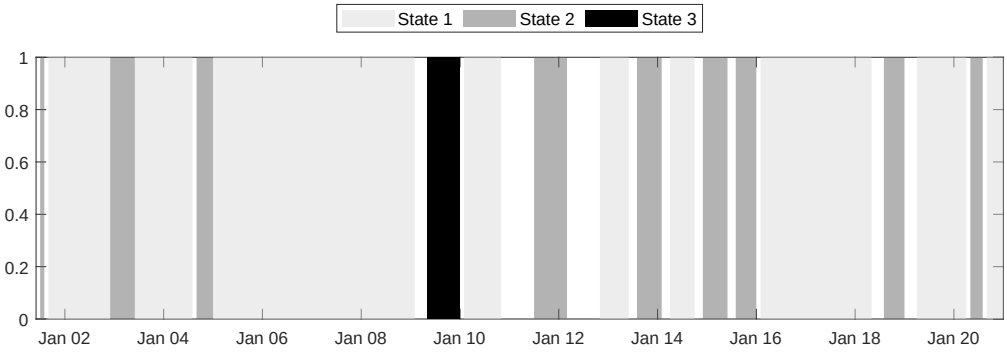

Figure 5: Time path of the model-implied three states obtained from the best-fitting state-switching model specification $\mathcal{M}_{3,3}$. This figure plots the shaded areas that highlight the periods of sample funds being in a particular model-implied state. Specifically, the light gray, dark gray, and black areas highlight respectively the periods of sample funds being in the *perverse timing* (the model-implied state $s_t = 1$), the *weakly positive timing* (the model-implied state $s_t = 2$) and the *strongly positive timing* (the model-implied state $s_t = 3$) states. The white area highlights the periods during which the model-implied states can not be determined as the probability of each state is less than a threshold of 50%. The sample period spans from July 2001 to December 2020.

Internet Appendix for "Optimal N-state endogenous Markov-switching model for currency liquidity timing"

Abstract

This internet appendix contains technical details and additional material on the robustness checks to the paper entitled "Optimal N-state endogenous Markov-switching model for currency liquidity timing". Appendix A provides the detailed derivation of the transition probabilities. Appendix B describes the simulation-based Bayesian inference procedure used to estimate the proposed model. Appendix C presents supporting tables and figures for the robustness checks.

February 1, 2025

Throughout the internet appendix, the following notations are adopted. Consider the N-state empirical form of our proposed model (11) and its variants in the paper, we let $y_t = R_t$ and $\mathbf{Y}_{\tau:t} = (y_\tau, ..., y_t)'$ collect the modeled fund return series between time τ and t; let $\mathbf{X}_{\tau:t} = (x_\tau, ..., x_t)'$ collect the input variables between time τ and t;[1] let β collect the coefficients[2] except the error term's variance σ^2; let $\mathbf{S}_{\tau:t} = (s_\tau, ..., s_t)'$ collect the latent Markov state variable between time τ and t; let $\mathbf{S}^*_{\tau:t} = (s^*_\tau, ..., s^*_t)'$ collect Hwu et al. (2021)'s random variables between time τ and t, with $s^*_t = (s^*_{1,t}, s^*_{2,t}, ..., s^*_{N-1,t})'$ (see (5) of the paper); let $\mathbf{Z}_{\tau:t} = (z_\tau, ..., z_t)'$ collect the transition covariates between time τ and t; let $\gamma = \{\gamma_{i,n}\}^{N-1,N}_{i=1,n=1}$, with $\gamma_{i,n} = (\{\bar{\gamma}_{i,n}\}^{N-1,N}_{i=1,n=1}, \{\gamma^z_{i,n}\}^{N-1,N}_{i=1,n=1})$ collecting the transition parameters (see (6) of the paper); let $\rho = \{\rho_i\}^{N-1}_{i=1}$ collect the transition parameters (see (6) of the paper); let $\theta = \{\beta, \gamma, \rho, \sigma^2\}$ collect all model parameters to be estimated (i.e., coefficients, transition parameters and error term's variance) in model specification (11) and its variants in the paper.

Appendix A. Transition probabilities

This section generalizes Hwu et al. (2021, Appendix B) for transition probabilities in the case of N states.

For $p_{n1,t}$ in (7) of the paper, we have

$$\begin{aligned} p_{n1,t} &= \Pr(s_t = 1 | s_{t-1} = n, z_t, \varepsilon_t) \\ &= \Pr(s^*_{1,t} < 0, s^*_{2,t} < 0, ..., s^*_{N-1,t} < 0) \\ &= \prod_{i=1}^{N-1} \Phi\left(\frac{-\bar{\gamma}_{i,s_{t-1}} - z_t' \gamma^z_{i,s_{t-1}} - \rho_i \varepsilon_t}{\sqrt{1-\rho_i^2}} \right), \end{aligned} \tag{A.1}$$

[1] For example $x_t = (1, \text{GMF}_t, \text{EMF}_t, \text{TERM}_t, \text{CREDIT}_t, \text{HML\_FX}_t, \text{RX}_t, (L^{\text{Cur}}_t - \bar{L}^{\text{Cur}})\text{HML\_FX}_t, (L^{\text{Cur}}_t - \bar{L}^{\text{Cur}})\text{RX}_t)'$ in (11) of the paper.

[2] For example $\beta = \{\alpha, \beta^{\text{GMF}}, \beta^{\text{EMF}}, \beta^{\text{TERM}}, \beta^{\text{CREDIT}}, \beta^{\text{HML\_FX}}, \beta^{\text{RX}}, \{\mu_n\}^N_{n=1}, \{\lambda_n\}^N_{n=1}\}$ in (11) of the paper.

for $n \in \{1, ..., N\}$; where $\Phi(\cdot)$ denotes the cumulative density function (CDF) of the standard normal distribution. For $p_{nj,t}$ in (7) of the paper, we have

$$\begin{aligned} p_{nj,t} &= \Pr(s_t = j | s_{t-1} = n, z_t, \varepsilon_t) \\ &= \Pr(s^*_{j-1,t} > 0, \{s^*_{j-1,t} - s^*_{m,t} > 0 : m = 1, ..., N-1, m \neq j-1\}) \\ &= F(0_{(N-1)\times 1} | c_{j-1,t}, V_{j-1}), \end{aligned} \tag{A.2}$$

for $n \in \{1, ..., N\}$ and $j \in \{2, ..., N\}$; where $F(\cdot | c_{j-1,t}, V_{j-1})$ denotes the CDF of the multivariate normal distribution with mean $c_{j-1,t}$ and variance-covariance V_{j-1}. We derive V_{j-1} as follows

$$V_{j-1} = \begin{pmatrix} 1-\rho^2_{j-1} & 1-\rho^2_{j-1} & \cdots & 1-\rho^2_{j-1} \\ 1-\rho^2_{j-1} & 2-\rho^2_{j-1}-\rho^2_1 & & \vdots \\ \vdots & & \ddots & 1-\rho^2_{j-1} \\ 1-\rho^2_{j-1} & \cdots & 1-\rho^2_{j-1} & 2-\rho^2_{j-1}-\rho^2_{N-1} \end{pmatrix},$$

and $c_{j-1,t}$ is given by

$$c_{j-1,t} = \begin{pmatrix} -\bar{\gamma}_{j-1,s_{t-1}} - z'_t \gamma^z_{j-1,s_{t-1}} - \rho_{j-1}\varepsilon_t \\ \bar{\gamma}_{1,s_{t-1}} - \bar{\gamma}_{j-1,s_{t-1}} + z'_t(\gamma^z_{1,s_{t-1}} - \gamma^z_{j-1,s_{t-1}}) + (\rho_1 - \rho_{j-1})\varepsilon_t \\ \vdots \\ \bar{\gamma}_{j-2,s_{t-1}} - \bar{\gamma}_{j-1,s_{t-1}} + z'_t(\gamma^z_{j-2,s_{t-1}} - \gamma^z_{j-1,s_{t-1}}) + (\rho_{j-2} - \rho_{j-1})\varepsilon_t \\ \bar{\gamma}_{j,s_{t-1}} - \bar{\gamma}_{j-1,s_{t-1}} + z'_t(\gamma^z_{j,s_{t-1}} - \gamma^z_{j-1,s_{t-1}}) + (\rho_j - \rho_{j-1})\varepsilon_t \\ \bar{\gamma}_{j+1,s_{t-1}} - \bar{\gamma}_{j-1,s_{t-1}} + z'_t(\gamma^z_{j+1,s_{t-1}} - \gamma^z_{j-1,s_{t-1}}) + (\rho_{j+1} - \rho_{j-1})\varepsilon_t \\ \vdots \\ \bar{\gamma}_{N-1,s_{t-1}} - \bar{\gamma}_{j-1,s_{t-1}} + z'_t(\gamma^z_{N-1,s_{t-1}} - \gamma^z_{j-1,s_{t-1}}) + (\rho_{N-1} - \rho_{j-1})\varepsilon_t \end{pmatrix}.$$

For variants of (7) of the paper, which are conditional on the information from z_t alone (see (12)–(13) of the paper), we have

$$\begin{aligned}
p_{n1,t} &= \Pr(s_t = 1 | s_{t-1} = n, z_t) \\
&= \Pr(s^*_{1,t} < 0, s^*_{2,t} < 0, ..., s^*_{N-1,t} < 0) \\
&= F(0_{(N-1)\times 1} | \bar{\gamma}_{s_{t-1}} + z_t' \gamma^z_{s_{t-1}}, \Omega) \\
p_{nj,t} &= \Pr(s_t = j | s_{t-1} = n, z_t) \\
&= \Pr(s^*_{j-1,t} > 0, \{s^*_{j-1,t} - s^*_{m,t} > 0 : m = 1, ..., N-1, m \neq j-1\}) \\
&= F(0_{(N-1)\times 1} | \bar{c}_{j-1,t}, \bar{V}_{j-1}),
\end{aligned} \tag{A.3}$$

for $n \in \{1, ..., N\}$ and $j \in \{2, ..., N\}$; where $\bar{\gamma}_{s_{t-1}}$ and $\gamma^z_{s_{t-1}}$ are defined in (B.8); Ω is defined in (B.9); the mean $\bar{c}_{j-1,t}$ is given by

$$c_{j-1,t} = \begin{pmatrix}
-\bar{\gamma}_{j-1,s_{t-1}} - z_t' \gamma^z_{j-1,s_{t-1}} \\
\bar{\gamma}_{1,s_{t-1}} - \bar{\gamma}_{j-1,s_{t-1}} + z_t'(\gamma^z_{1,s_{t-1}} - \gamma^z_{j-1,s_{t-1}}) \\
\vdots \\
\bar{\gamma}_{j-2,s_{t-1}} - \bar{\gamma}_{j-1,s_{t-1}} + z_t'(\gamma^z_{j-2,s_{t-1}} - \gamma^z_{j-1,s_{t-1}}) \\
\bar{\gamma}_{j,s_{t-1}} - \bar{\gamma}_{j-1,s_{t-1}} + z_t'(\gamma^z_{j,s_{t-1}} - \gamma^z_{j-1,s_{t-1}}) \\
\bar{\gamma}_{j+1,s_{t-1}} - \bar{\gamma}_{j-1,s_{t-1}} + z_t'(\gamma^z_{j+1,s_{t-1}} - \gamma^z_{j-1,s_{t-1}}) \\
\vdots \\
\bar{\gamma}_{N-1,s_{t-1}} - \bar{\gamma}_{j-1,s_{t-1}} + z_t'(\gamma^z_{N-1,s_{t-1}} - \gamma^z_{j-1,s_{t-1}})
\end{pmatrix},$$

and the variance-covariance $\bar{V}_{j-1}$ is formulated as

$$\bar{V}_{j-1} = \begin{pmatrix} 1 & 1-\rho_1\rho_{j-1} & \cdots & 1-\rho_{N-1}\rho_{j-1} \\ 1-\rho_1\rho_{j-1} & 2(1-\rho_1\rho_{j-1}) & & \vdots \\ \vdots & & \ddots & 1+\rho_{N-1}\rho_{N-2} \\ & & & -\rho_{N-1}\rho_{j-1}-\rho_{N-2}\rho_{j-1} \\ 1-\rho_{N-1}\rho_{j-1} & \cdots & 1+\rho_{N-1}\rho_{N-2} & 2(1-\rho_{N-1}\rho_{j-1}) \\ & & -\rho_{N-1}\rho_{j-1}-\rho_{N-2}\rho_{j-1} & \end{pmatrix}.$$

Appendix B. Simulation-based Bayesian inference procedure

This section provides the computational details (i.e., priors, conditional posterior distributions, sampling algorithms, and marginal likelihoods) of the simulation-based Bayesian inference procedure used to estimate the empirical form of our proposed model (11) and its variants in the paper.

B.1. Priors

In Table A.1, we specify a standard set of independent priors on model parameters $\theta = \{\beta, \gamma, \rho, \sigma^2\}$ as with Kim and Kang (2022).

Table A.1: Priors

Parameter	Priors	Hyperparameters
β	$\mathcal{N}(\bar{\beta}, \bar{V}_\beta)$	$\bar{\beta} = 0_{K\times 1}$, $\bar{V}_\beta = I_K$
γ	$\mathcal{N}(\bar{\Gamma}_i, \bar{V}_{\Gamma_i})$	N = 2: $\bar{\Gamma}_1 = (\bar{\gamma}_{1,1}, \gamma^z_{1,1}, \bar{\gamma}_{1,2}, \gamma^z_{1,2})'$ = (-1.5, 0, 1.5, 0)', $\bar{V}_{\Gamma_1} = I_N \otimes$ diag(0.05,0.1)
		N = 3: $\bar{\Gamma}_1 = (\bar{\gamma}_{1,1}, \gamma^z_{1,1}, \bar{\gamma}_{1,2}, \gamma^z_{1,2}, \bar{\gamma}_{1,3}, \gamma^z_{1,3})'$ = (-1.5, 0 1.5, 0, 0, 0)', $\bar{V}_{\Gamma_1} = I_N \otimes$ diag(0.05,0.1)
		$\bar{\Gamma}_2 = (\bar{\gamma}_{2,1}, \gamma^z_{2,1}, \bar{\gamma}_{2,2}, \gamma^z_{2,2}, \bar{\gamma}_{2,3}, \gamma^z_{2,3})'$ = (-2, 0, -0.5, 0, 1.5, 0)', $\bar{V}_{\Gamma_2} = I_N \otimes$ diag(0.05,0.1)
		N = 4: $\bar{\Gamma}_1 = (\bar{\gamma}_{1,1}, \gamma^z_{1,1}, \bar{\gamma}_{1,2}, \gamma^z_{1,2}, \bar{\gamma}_{1,3}, \gamma^z_{1,3}, \bar{\gamma}_{1,4}, \gamma^z_{1,4})'$ = (-2.5, 0, 1.5, 0, -1.5, 0, 0, 0)', $\bar{V}_{\Gamma_1} = I_N \otimes$ diag(0.05,0.1)
		$\bar{\Gamma}_2 = (\bar{\gamma}_{2,1}, \gamma^z_{2,1}, \bar{\gamma}_{2,2}, \gamma^z_{2,2}, \bar{\gamma}_{2,3}, \gamma^z_{2,3}, \bar{\gamma}_{2,4}, \gamma^z_{2,4})'$ = (-2, 0, 0.5, 0, 1.5, 0, -0.5, 0)', $\bar{V}_{\Gamma_2} = I_N \otimes$ diag(0.05,0.1)
		$\bar{\Gamma}_3 = (\bar{\gamma}_{3,1}, \gamma^z_{3,1}, \bar{\gamma}_{3,2}, \gamma^z_{3,2}, \bar{\gamma}_{3,3}, \gamma^z_{3,3}, \bar{\gamma}_{3,4}, \gamma^z_{3,4})'$ = (-1.5, 0, 0, 0, -0.5, 0, 1.5, 0)', $\bar{V}_{\Gamma_3} = I_N \otimes$ diag(0.05,0.1)
$0.5 \times (\rho_i + 1)$	$Beta(a_0, b_0)$	$a_0 = 4$, $b_0 = 4$
σ^2	$\mathcal{IG}(\nu_0, R_0)$	$\nu_0 = R_0/\hat{s} + 1$, $R_0 = \hat{s}(\hat{s}^2/\sigma^2_{\hat{s}}) + 1$

NOTES: This table presents a standard set of independent priors on model parameters $\theta = \{\beta, \gamma, \rho, \sigma^2\}$ as with Kim and Kang (2022). $\mathcal{N}(a, b)$ denotes the Normal distribution with mean a and variance b; $Beta(a, b)$ denotes the Beta distribution with shape parameters a and b; $\mathcal{IG}(a, b)$ denotes the Inverse Gamma distribution with shape parameter a and scale parameter b. The priors depend on the set of hyperparameters $(\bar{\beta}, \bar{V}_\beta, \{\bar{\Gamma}_i\}_{i=1}^{N-1}, \{\bar{V}_{\Gamma_i}\}_{i=1}^{N-1}, a_0, b_0, \nu_0, R_0)$.

The prior on β is assumed to be Gaussian with mean $\bar{\beta}$ and variance $\bar{V}_\beta$. We set the hyperparameters $\bar{\beta}$ and $\bar{V}_\beta$ to be weakly informative such that the impact of the prior on the

posterior distribution is limited. Specifically, we set $\bar{\beta} = 0_{K\times 1}$ and $\bar{V}_\beta = I_K$, where $0_{K\times 1}$ is a K-dimensional vector of zeros, I_K is a $K \times K$ identity matrix and K denotes the number of coefficients collected in β.

The priors on $\gamma = \{\gamma_{i,n}\}_{i=1,n=1}^{N-1,N}$ are assumed to be Gaussian. Specifically, for $i = 1, 2, ..., N-1$, we assume the vector $(\gamma_{i,n=1}, \gamma_{i,n=2}, ..., \gamma_{i,n=N})'$ is normally distributed with mean $\bar{\Gamma}_i$ and variance $\bar{V}_{\Gamma_i}$. In our empirical analysis where $N = 2, 3, 4$ is considered (see Section 4.2 in the paper), we set the hyperparameters $\bar{\Gamma}_i$ and $\bar{V}_{\Gamma_i}$ in each case of N to be uninformative as in Kim and Kang (2022).

The priors on $\rho = \{\rho_i\}_{i=1}^{N-1}$ are assumed to be Beta with shape parameters a_0 and b_0. The hyperparameters a_0 and b_0 are set to allow the prior mean of ρ_i (transformed from $0.5 \times (\rho_i + 1)$) to be zero, which is uninformative as suggested by Kim and Kang (2022).

The prior on σ^2 is assumed to be Inverse Gamma with shape parameter ν_0 and scale parameter R_0. The hyperparameters ν_0 and R_0 are formulated to allow the prior mean of σ^2 to be concentrated around the OLS estimate of the error term's variance, i.e., $\nu_0 = R_0/\hat{s} + 1$, $R_0 = \hat{s}(\hat{s}^2/\sigma_{\hat{s}}^2) + 1$, where $\hat{s}^2$ denotes the error term's variance estimated from OLS and $\sigma_{\hat{s}}^2$ denotes the variance of $\hat{s}$. We set $\sigma_{\hat{s}}^2$ to 0.25, which seems to reflect an ex ante plausible range for the values of $\hat{s}$.

B.2. Conditional posterior distributions and sampling algorithms

Let $\theta_{-\beta}$ denote the collection of model parameters, excluding β. Similarly, let $\theta_{-\gamma}$, $\theta_{-\rho}$, and $\theta_{-\sigma^2}$ denote the collections of model parameters except γ, ρ, and σ^2, respectively. To obtain posterior samples of the latent variables $\mathbf{S}_{1:T}$ and $\mathbf{S}^*_{1:T}$ as well as the model parameters $\theta = \{\beta, \gamma, \rho, \sigma^2\}$, we adopt a simulation-based Bayesian inference procedure that iterates between the following steps

Step 1: sampling $\mathbf{S}_{1:T}$ given $\mathbf{Y}_{1:T}, \mathbf{X}_{1:T}, \mathbf{Z}_{1:T}, \theta$.

Step 2: sampling $\mathbf{S}^*_{1:T}$ given $\mathbf{S}_{1:T}, \mathbf{Y}_{1:T}, \mathbf{X}_{1:T}, \mathbf{Z}_{1:T}, \theta$.

Step 3: sampling β given $\mathbf{S}_{1:T}, \mathbf{S}^*_{1:T}, \mathbf{Y}_{1:T}, \mathbf{X}_{1:T}, \mathbf{Z}_{1:T}, \theta_{-\beta}$.

Step 4: sampling γ given $\mathbf{S}_{1:T}, \mathbf{S}^*_{1:T}, \mathbf{Y}_{1:T}, \mathbf{Z}_{1:T}, \theta_{-\gamma}$.

Step 5: sampling ρ given $\mathbf{S}_{1:T}, \mathbf{S}^*_{1:T}, \mathbf{Y}_{1:T}, \mathbf{X}_{1:T}, \mathbf{Z}_{1:T}, \theta_{-\rho}$.

Step 6: sampling σ^2 given $\mathbf{S}_{1:T}, \mathbf{S}^*_{1:T}, \mathbf{Y}_{1:T}, \mathbf{X}_{1:T}, \mathbf{Z}_{1:T}, \theta_{-\sigma^2}$.

Throughout the paper, we conduct 150,000 iterations of the above sampling procedure. To mitigate the dependence on the initial posterior samples and reduce the serial correlation among the posterior samples, we discard the first 25,000 iterations as burn-in and thin the remaining 125,000 iterations at an interval of 10. This finally leaves 12,500 posterior samples from which we derive the posterior summary of the estimated model parameters. We now provide the details of each step as follows.

Sampling $\mathbf{S}_{1:T}$. We sample the whole path $\mathbf{S}_{1:T}$ from its conditional posterior distribution based on a forward-filtering backward-sampling (FFBS) algorithm. The FFBS algorithm consists of two stages. In the first stage, we carry out a forward recursion to obtain the filtered probability. In the second stage, we compute the conditional posterior distribution of $\mathbf{S}_{1:T}$ using the filtered probabilities, and randomly draw $\mathbf{S}_{1:T}$ from its conditional posterior distribution through a backward recursion. We implement the FFBS algorithm following Kim and Kang (2022, Appendix A.1).

Sampling $\mathbf{S}^*_{1:T}$. We sample each s^*_t collected in $\mathbf{S}^*_{1:T}$ from its conditional posterior distribution $p(s^*_t|s_t, s_{t-1}, \mathbf{Y}_{1:T}, \mathbf{X}_{1:T}, \mathbf{Z}_{1:T}, \theta)$ independently for $t = 1, ..., T$. Recall that $s^*_t = (s^*_{1,t}, s^*_{2,t}, ..., s^*_{N-1,t})'$, each of which is mutually uncorrelated according to Hwu et al. (2021). Thus, the conditional posterior distribution $p(s^*_t|s_t, s_{t-1}, \mathbf{Y}_{1:T}, \mathbf{X}_{1:T}, \mathbf{Z}_{1:T}, \theta)$ is simply given by the product of $\left\{p(s^*_{i,t}|s_t, s_{t-1}, \mathbf{Y}_{1:T}, \mathbf{X}_{1:T}, \mathbf{Z}_{1:T}, \theta)\right\}_{i=1}^{N-1}$, which following (5)–(6) in the pa-

per is proportional to

$$\begin{aligned}&\mathcal{N}(s^*_{i,t}|\bar{\gamma}_{i,s_{t-1}} + z'_t\gamma^z_{i,s_{t-1}} + \rho_i\varepsilon_t, 1-\rho_i^2)\times \\ &[\mathbf{I}(s^*_{i,t} > s^*_{h,t}|s_t)\Pr(\mathbf{I}(s^*_{i,t} > s^*_{h,t}|s_t)) + \mathbf{I}(s^*_{i,t} \leq s^*_{h,t}|s_t)\Pr(\mathbf{I}(s^*_{i,t} \leq s^*_{h,t}|s_t))],\end{aligned} \tag{B.1}$$

for $h = 0, 1, ..., i-1, i+1, ..., N-1$; where $s^*_{0,t} = 0$; $\mathbf{I}(\cdot)$ is an indicator function. From (5) in the paper, (B.1) has different functional forms depending on the realization of s_t. Consider the case that $s_t = 1$, all random variables are negative. This reflects in (B.1) that $\mathbf{I}(s^*_{i,t} > s^*_{0,t}|s_t) = 0$, $\Pr(\mathbf{I}(s^*_{i,t} > s^*_{0,t}|s_t)) = 0$, $\mathbf{I}(s^*_{i,t} \leq s^*_{0,t}|s_t) = 1$, and $\Pr(\mathbf{I}(s^*_{i,t} \leq s^*_{0,t}|s_t)) = 1$ for $i = 1, 2, ..., N-1$. Thus, (B.1) for any given random variable $s^*_{i,t}$ can be rewritten as

$$\mathcal{N}(s^*_{i,t}|\bar{\gamma}_{i,s_{t-1}} + z'_t\gamma^z_{i,s_{t-1}} + \rho_i\varepsilon_t, 1-\rho_i^2) \times \mathbf{I}(s^*_{i,t} \leq s^*_{0,t}|s_t), \tag{B.2}$$

and indicates that $s^*_{i,t}$ can be sampled from the truncated normal distributions over $(-\infty,0]$

$$s^*_{i,t} \sim \mathcal{TN}_{(-\infty,0]}(\bar{\gamma}_{i,s_{t-1}} + z'_t\gamma^z_{i,s_{t-1}} + \rho_i\varepsilon_t, 1-\rho_i^2). \tag{B.3}$$

Consider the case that $2 \leq s_t = i+1 \leq N$, the i-th random variable $s^*_{i,t}$ is positive. Thus, (B.1) for $s^*_{i,t}$ can be rewritten as

$$\mathcal{N}(s^*_{i,t}|\bar{\gamma}_{i,s_{t-1}} + z'_t\gamma^z_{i,s_{t-1}} + \rho_i\varepsilon_t, 1-\rho_i^2) \times \mathbf{I}(s^*_{i,t} > s^*_{0,t}|s_t), \tag{B.4}$$

and indicates that $s^*_{i,t}$ can be sampled from the truncated normal distributions over $(0, \infty]$

$$s^*_{i,t} \sim \mathcal{TN}_{(0,\infty]}(\bar{\gamma}_{i,s_{t-1}} + z'_t\gamma^z_{i,s_{t-1}} + \rho_i\varepsilon_t, 1-\rho_i^2). \tag{B.5}$$

Besides, the i-th random variable $s^*_{i,t}$ should be larger than the other random variables.

Thus, given the sample of $s^*_{i,t}$, (B.1) for the remaining random variables can be rewritten as

$$\mathcal{N}(s^*_{h,t}|\bar{\gamma}_{h,s_{t-1}} + z'_t\gamma^z_{h,s_{t-1}} + \rho_h\varepsilon_t, 1-\rho_h^2) \times \mathbf{I}(s^*_{h,t} < s^*_{i,t}|s_t), \tag{B.6}$$

for $h = 1, 2, ..., j-1, j+1, ..., N-1$, and indicates that $s^*_{h,t}$ can be sampled from the truncated normal distributions over $(-\infty, s^*_{i,t}]$

$$s^*_{h,t} \sim \mathcal{TN}_{(-\infty, s^*_{i,t}]}(\bar{\gamma}_{h,s_{t-1}} + z'_t\gamma^z_{h,s_{t-1}} + \rho'_h\varepsilon_t, 1-\rho_h^2). \tag{B.7}$$

This completes the sampling of each s^*_t collected in $\mathbf{S}^*_{1:T}$.

Sampling β. We sample β from its conditional posterior distribution, which is given by

$$\beta|\mathbf{S}_{1:T}, \mathbf{S}^*_{1:T}, \mathbf{Y}_{1:T}, \mathbf{X}_{1:T}, \mathbf{Z}_{1:T}, \theta_{-\beta} \sim \mathcal{N}(B_1 A, B_1), \tag{B.8}$$

with $B_1 = (\bar{V}_\beta^{-1} + \sum_{t=1}^T X_t(\sigma(1-\rho'\Omega^{-1}\rho)\sigma')^{-1}X'_t)^{-1}$, $A = (\bar{V}_\beta^{-1}\bar{\beta} + \sum_{t=1}^T X_t(\sigma(1-\rho'\Omega^{-1}\rho)\sigma')^{-1}y^*_t)$ and $X_t = [(\mathbf{I}(s_t = 1)\ \mathbf{I}(s_t = 2)\ \cdots\ \mathbf{I}(s_t = N)) \otimes x'_t]'$; where $y^*_t = y_t - \sigma\rho'\Omega^{-1}(s^*_t - \bar{\gamma}_{s_{t-1}} - z'_t\gamma^z_{s_{t-1}})$, $\bar{\gamma}_{s_{t-1}} = (\bar{\gamma}_{1,s_{t-1}}, \bar{\gamma}_{2,s_{t-1}}, ..., \bar{\gamma}_{N-1,s_{t-1}})'$, $\gamma^z_{s_{t-1}} = (\gamma^z_{1,s_{t-1}}, \gamma^z_{2,s_{t-1}}, ..., \gamma^z_{N-1,s_{t-1}})'$ and

$$\Omega = \begin{pmatrix} 1 & \rho_1\rho_2 & \cdots & \rho_1\rho_{N-1} \\ \rho_2\rho_1 & 1 & & \vdots \\ \vdots & & \ddots & \rho_{N-2}\rho_{N-1} \\ \rho_{N-1}\rho_1 & \cdots & \rho_{N-1}\rho_{N-2} & 1 \end{pmatrix}. \tag{B.9}$$

Sampling γ. For each $i = 1, 2, ..., N-1$, we sample $(\gamma_{i,n=1}, \gamma_{i,n=2}, ..., \gamma_{i,n=N})'$ from its

conditional posterior distribution, which is given by

$$(\gamma_{i,n=1}, \gamma_{i,n=2}, ..., \gamma_{i,n=N})' | \mathbf{S}_{1:T}, \mathbf{S}^*_{1:T}, \mathbf{Y}_{1:T}, \mathbf{Z}_{1:T}, \theta_{-\gamma} \sim \mathcal{N}(B_{i,1} A_i, B_{i,1}), \tag{B.10}$$

with $B_{i,1} = (\sum_{t=1}^{T} (1-\rho_i^2)^{-1} \mathbf{I}_t \mathbf{I}_t' + \bar{V}_{\Gamma_i}^{-1})^{-1}$, $A_i = (\sum_{t=1}^{T} (1-\rho_i^2)^{-1} \mathbf{I}_t (s^*_{i,t} - \rho_i \varepsilon_t) + \bar{V}_{\Gamma_i}^{-1} \bar{\Gamma}_i)$ and $\mathbf{I}_t = [(\mathbf{I}(s_{t-1}=1)\ \mathbf{I}(s_{t-1}=2)\ \cdots\ \mathbf{I}(s_{t-1}=N)) \otimes x_t']'$.

Sampling ρ. We sample ρ from its conditional posterior distribution, which is proportional to $p(\mathbf{S}^*_{1:T}, \mathbf{Y}_{1:T} | \mathbf{S}_{1:T}, \mathbf{X}_{1:T}, \mathbf{Z}_{1:T}, \theta) \times \pi(\rho)$. Since $p(\mathbf{S}^*_{1:T}, \mathbf{Y}_{1:T} | \mathbf{S}_{1:T}, \mathbf{X}_{1:T}, \mathbf{Z}_{1:T}, \theta)$ is not standard, we implement a Metropolis-Hastings (MH) algorithm similar to Kim and Kang (2022, Algorithm 4).

Sampling σ^2. We sample σ^2 from its conditional posterior distribution, which is proportional to $p(\mathbf{Y}_{1:T} | \mathbf{S}_{1:T}, \mathbf{S}^*_{1:T}, \mathbf{X}_{1:T}, \mathbf{Z}_{1:T}, \theta) \times \mathcal{IG}(\sigma^2 | \nu_0, R_0)$. Since $p(\mathbf{Y}_{1:T} | \mathbf{S}_{1:T}, \mathbf{S}^*_{1:T}, \mathbf{X}_{1:T}, \mathbf{Z}_{1:T}, \theta)$ is not standard, we implement a Metropolis-Hastings (MH) algorithm similar to Kim and Kang (2022, Algorithm 5).

B.3. Marginal likelihoods

The marginal likelihood (in logarithm) of a given model specification $\mathcal{M}_{R,N}$ in Section 4.2 of the paper, denoted by $\log p(\mathbf{Y}_{1:T} | \mathcal{M}_{R,N})$, is computed as

$$\log p(\mathbf{Y}_{1:T} | \mathcal{M}_{R,N}) = \log p(\mathbf{Y}_{1:T} | \hat{\theta}, \mathcal{M}_{R,N}) + \log \pi(\hat{\theta} | \mathcal{M}_{R,N}) - \log \pi(\hat{\theta} | \mathbf{Y}_{1:T}, \mathcal{M}_{R,N}), \tag{B.11}$$

where $\hat{\theta} = (\hat{\beta}, \hat{\gamma}, \hat{\rho}, \hat{\sigma}^2)$ is the posterior mode. According to Kim and Kang (2022), the calculation of the likelihood $\log p(\mathbf{Y}_{1:T} | \hat{\theta}, \mathcal{M}_{R,N})$ and prior density at the mode $\log \pi(\hat{\theta} | \mathcal{M}_{R,N})$ is straightforward. In contrast, the log posterior density $\log \pi(\hat{\theta} | \mathbf{Y}_{1:T}, \mathcal{M}_{R,N})$ is computationally challenging, because this is not analytical. Here, we follow Chib and Jeliazkov (2001)

and decompose the log posterior density into four log conditional densities, as

$$\begin{aligned}\log \pi(\hat{\theta}|\mathbf{Y}_{1:T}, \mathcal{M}_{R,N}) = &\log \pi(\hat{\beta}|\mathbf{Y}_{1:T}, \hat{\theta}_{-\beta}, \mathcal{M}_{R,N}) + \log \pi(\hat{\gamma}|\mathbf{Y}_{1:T}, \hat{\sigma}^2, \hat{\rho}, \mathcal{M}_{R,N}) \\ &+ \log \pi(\hat{\rho}|\mathbf{Y}_{1:T}, \hat{\sigma}^2, \mathcal{M}_{R,N}) + \log \pi(\hat{\sigma}^2|\mathbf{Y}_{1:T}, \mathcal{M}_{R,N}),\end{aligned} \tag{B.12}$$

and compute each of them in parallel. We now provide the computational details of each term in (B.12) as follows.

Computing $\pi(\hat{\beta}|\mathbf{Y}_{1:T}, \hat{\theta}_{-\beta}, \mathcal{M}_{R,N})$. This can be approximated numerically as

$$\pi(\hat{\beta}|\mathbf{Y}_{1:T}, \hat{\theta}_{-\beta}, \mathcal{M}_{R,N}) \approx n_1^{-1} \sum_{g=1}^{n_1} \mathcal{N}(\hat{\beta}|B_1^{(g)} A^{(g)}, B_1^{(g)}), \tag{B.13}$$

with $B_1^{(g)} = (\bar{V}_\beta^{-1} + \sum_{t=1}^T X_t(\hat{\sigma}(1 - \hat{\rho}'\Omega^{-1}\hat{\rho})\hat{\sigma}')^{-1}X_t')^{-1}$, $A^{(g)} = (\bar{V}_\beta^{-1}\bar{\beta} + \sum_{t=1}^T X_t(\hat{\sigma}(1 - \hat{\rho}'\Omega^{-1}\hat{\rho})\hat{\sigma}')^{-1}y_t^{*,(g)})$, and $X_t = [(\mathbf{I}(s_t = 1)\ \mathbf{I}(s_t = 2)\ \cdots\ \mathbf{I}(s_t = N)) \otimes x_t']'$; where Ω is defined in (B.9); $y_t^{*,(g)} = y_t - \hat{\sigma}\hat{\rho}'\hat{\Omega}^{-1}(s_t^{*,(g)} - \bar{\gamma}_{s_{t-1}^{(g)}} - z_t'\gamma^z_{s_{t-1}^{(g)}})$; the superscript (g) denotes the g-th posterior sample and n_1 denotes the number of iterations; $(\beta, \mathbf{S}_{1:T}, \mathbf{S}^*_{1:T})$ are sampled but (γ, ρ, σ^2) are fixed at their mode, $(\hat{\gamma}, \hat{\rho}, \hat{\sigma}^2)$.

Computing $\log \pi(\hat{\gamma}|\mathbf{Y}_{1:T}, \hat{\sigma}^2, \hat{\rho}, \mathcal{M}_{R,N})$. This can be approximated numerically as

$$\pi(\hat{\gamma}|\mathbf{Y}_{1:T}, \hat{\sigma}^2, \hat{\rho}, \mathcal{M}_{R,N}) \approx n_1^{-1} \sum_{g=1}^{n_1} \mathcal{N}(\hat{\gamma}|B_{i,1}^{(g)} A_i^{(g)}, B_{i,1}^{(g)}), \tag{B.14}$$

with $B_{i,1}^{(g)} = (\sum_{t=1}^T (1 - \hat{\rho}_i^2)^{-1}\mathbf{I}_t\mathbf{I}_t' + \bar{V}_{\Gamma_i}^{-1})^{-1}$, $A_i^{(g)} = (\sum_{t=1}^T (1 - \hat{\rho}_i^2)^{-1}\mathbf{I}_t(s_{i,t}^{*,(g)} - \hat{\rho}_i\varepsilon_t^{(g)}) + \bar{V}_{\Gamma_i}^{-1}\bar{\Gamma}_i)$ and $\mathbf{I}_t = [(\mathbf{I}(s_{t-1} = 1)\ \mathbf{I}(s_{t-1} = 2)\ \cdots\ \mathbf{I}(s_{t-1} = N)) \otimes x_t']'$; where $\varepsilon_t^{(g)} = \hat{\sigma}^{-1}(y_t - x_t'\beta^{(g)}_{s_t^{(g)}})$; $(\gamma, \beta, \mathbf{S}_{1:T}, \mathbf{S}^*_{1:T})$ are sampled but (ρ, σ^2) are fixed at their mode, $(\hat{\rho}, \hat{\sigma}^2)$.

Computing $\pi(\hat{\rho}|\mathbf{Y}_{1:T}, \hat{\sigma}^2, \mathcal{M}_{R,N})$. This can computed from the MH output in a multiple-block sampling framework, using the method similar to Kim and Kang (2022, Appendix

B.3).

Computing $\pi(\hat{\sigma}^2|\mathbf{Y}_{1:T}, \mathcal{M}_{R,N})$. This can computed from the MH output in a multiple-block sampling framework, using the method similar to Kim and Kang (2022, Appendix B.4).

Appendix C. Additional material on the robustness checks

This section presents supporting tables and figures discussed in Section 5 of the paper.

Table C.1: Estimation results: Robustness 1

	s_t/s_{t-1}	Mean	s.e.	95% HPDI		Ineff	p-val
Panel A: Non-state-switching coefficients							
α (%)		0.093	0.056	[-0.013,	0.209]	67.796	0.616
β^{GMF}		0.094	0.025	[0.027,	0.122]	62.741	0.601
β^{EMF}		0.059	0.013	[0.019,	0.069]	57.632	0.607
β^{TERM}		1.581	0.247	[1.129,	2.079]	66.398	0.614
β^{CREDIT}		0.106	0.034	[0.053,	0.184]	67.802	0.541
$\beta^{\text{HML\_FX}}$		0.033	0.021	[-0.008,	0.047]	70.074	0.072
β^{RX}		0.140	0.018	[0.130,	0.182]	65.711	0.217
$\psi^{\text{HML\_FX}}$		-1.422	0.349	[-1.653,	-0.516]	64.826	0.574
ψ^{RX}		-0.216	0.516	[-1.254,	0.171]	65.589	0.351
$\delta^{\text{HML\_FX}}$		-0.113	0.145	[-0.448,	0.049]	64.781	0.465
δ^{RX}		0.033	0.199	[-0.095,	0.469]	69.850	0.093
σ		0.004	0.000	[0.004,	0.005]	12.100	0.950
Panel B: Currency-liquidity-timing coefficients							
μ_{s_t}	1	0.075	0.081	[-0.107,	0.120]	65.196	0.230
	2	0.142	0.087	[-0.026,	0.311]	63.225	0.695
	3	0.544	0.205	[0.087,	0.798]	69.615	0.306
λ_{s_t}	1	-0.870	0.427	[-1.130,	0.118]	71.188	0.149
	2	0.610	0.254	[0.035,	1.009]	63.467	0.892
	3	1.264	0.407	[0.714,	2.497]	62.678	0.628
Panel C: Transition parameters							
$\bar{\gamma}_{1,s_{t-1}}$	1	-1.366	0.212	[-1.780,	-0.957]	12.591	0.120
	2	1.178	0.199	[0.789,	1.567]	4.546	0.526
	3	-0.134	0.208	[-0.532,	0.275]	2.053	0.618
$\gamma^z_{1,s_{t-1}}$	1	0.102	0.288	[-0.481,	0.652]	17.813	0.202
	2	-0.301	0.274	[-0.846,	0.227]	9.110	0.772
	3	-0.165	0.292	[-0.739,	0.403]	2.130	0.647
$\bar{\gamma}_{2,s_{t-1}}$	1	-1.974	0.223	[-2.399,	-1.530]	6.009	0.462
	2	-0.637	0.203	[-1.016,	-0.225]	3.691	0.053
	3	1.270	0.213	[0.846,	1.680]	3.210	0.470
$\gamma^z_{2,s_{t-1}}$	1	-0.093	0.292	[-0.665,	0.473]	4.841	0.139
	2	-0.237	0.277	[-0.771,	0.319]	4.293	0.320
	3	-0.305	0.288	[-0.889,	0.240]	2.622	0.097
ρ_1		-0.315	0.252	[-0.717,	0.221]	44.187	0.193
ρ_2		0.011	0.238	[-0.469,	0.444]	16.746	0.363
Panel D: State differences in currency-liquidity-timing coefficients							
$\mu_2 - \mu_1$		0.067	0.057	[0.029,	0.211]	61.949	0.425
$\mu_3 - \mu_2$		0.402	0.183	[0.033,	0.679]	70.899	0.383
$\lambda_2 - \lambda_1$		1.481	0.433	[0.486,	1.762]	70.342	0.088
$\lambda_3 - \lambda_2$		0.654	0.403	[0.113,	1.498]	66.065	0.548

NOTES: This table presents the posterior summary of the best-fitting state-switching model specification $\mathcal{M}_{3,3}$ with controls for currency return and volatility timing, including the posterior means (Mean), the posterior standard errors (s.e.), 95% highest posterior density interval (95% HPDI), inefficiency factor (Ineff) and Geweke (1992)'s p-value (p-val) of the obtained parameters' posterior samples. The model specification is given by

$$R_t = \alpha + \beta^{\text{HML\_FX}}\text{HML\_FX}_t + \mu_{s_t}(L_t^{\text{Cur}} - \bar{L}^{\text{Cur}})\text{HML\_FX}_t + \beta^{\text{RX}}\text{RX}_t + \lambda_{s_t}(L_t^{\text{Cur}} - \bar{L}^{\text{Cur}})\text{RX}_t + \psi^{\text{HML\_FX}}\text{HML\_FX}_t^2$$
$$+ \psi^{\text{RX}}\text{RX}_t^2 + \delta^{\text{HML\_FX}}(\sigma_t^{\text{Cur}} - \bar{\sigma}^{\text{Cur}})\text{HML\_FX}_t + \delta^{\text{RX}}(\sigma_t^{\text{Cur}} - \bar{\sigma}^{\text{Cur}})\text{RX}_t + \sum_{j=1}^{4}\beta^j f_t^j + \varepsilon_t,$$

where t denotes a month; $s_t \in \{1, 2, 3\}$ and the associated state transitions are formulated by (5)–(7) of the paper; R_t is the equally weighted return of all sample funds; HML_FX_t and RX_t are the risk factors specific to the currency market—the carry-trade and the dollar factors; $\{f_t^j\}_{j=1}^4 = \{\text{GMF}_t, \text{EMF}_t, \text{TERM}_t, \text{CREDIT}_t\}$ are the additional risk factors—the hedged global bond market factor, the emerging bond market factor, the term factor, and the credit factor; L_t^{Cur} is the systematic currency liquidity and $\bar{L}^{\text{Cur}}$ its historical average; σ_t^{Cur} is the systematic currency volatility constructed in Menkhoff et al. (2012) and $\bar{\sigma}^{\text{Cur}}$ its historical average; μ_{s_t} and λ_{s_t} are currency-liquidity-timing coefficients; $\psi^{\text{HML\_FX}}$ and ψ^{RX} are currency-return-timing coefficients; $\delta^{\text{HML\_FX}}$ and δ^{RX} are currency-volatility-timing coefficients. Results are based on a simulation-based Bayesian inference procedure with 12,500 iterations. The sample period spans from July 2001 to December 2020.

Table C.2: Estimation results: Robustness 2

	s_t/s_{t-1}	Mean	s.e.	95% HPDI		Ineff	p-val
Panel A: Non-state-switching coefficients							
α (%)		0.049	0.007	[0.044,	0.049]	53.281	0.937
β^{GMF}		0.110	0.014	[0.071,	0.113]	71.062	0.750
β^{EMF}		0.065	0.008	[0.067,	0.071]	72.798	0.776
β^{TERM}		1.495	0.045	[1.497,	1.504]	66.598	0.751
β^{CREDIT}		0.098	0.008	[0.070,	0.100]	69.139	0.703
$\beta^{\text{HML\_FX}}$		0.020	0.014	[0.016,	0.067]	73.609	0.586
β^{RX}		0.146	0.006	[0.145,	0.145]	69.095	0.827
$\psi^{\text{HML\_FX}}$		-0.071	0.038	[-0.199,	-0.065]	71.733	0.822
ψ^{RX}		0.107	0.019	[0.050,	0.112]	66.746	0.625
σ		0.004	0.000	[0.004,	0.005]	20.831	0.540
Panel B: Currency-liquidity-timing coefficients							
μ_{s_t}	1	0.033	0.349	[-0.930,	0.154]	74.053	0.542
	2	0.238	0.270	[-0.394,	0.328]	72.121	0.566
	3	0.382	0.098	[0.352,	0.677]	70.956	0.598
λ_{s_t}	1	-1.136	0.104	[-1.145,	-0.807]	64.076	0.882
	2	-0.060	0.297	[-0.154,	0.753]	72.767	0.586
	3	2.086	0.371	[0.831,	2.210]	73.605	0.559
Panel C: Transition parameters							
$\bar{\gamma}_{1,s_{t-1}}$	1	-1.531	0.211	[-1.936,	-1.106]	3.903	0.589
	2	1.299	0.205	[0.912,	1.708]	2.071	0.631
	3	-0.134	0.207	[-0.532,	0.280]	0.964	0.998
$\gamma^z_{1,s_{t-1}}$	1	-0.036	0.285	[-0.598,	0.517]	3.023	0.826
	2	-0.272	0.281	[-0.823,	0.273]	2.023	0.867
	3	-0.129	0.289	[-0.684,	0.452]	1.031	0.951
$\bar{\gamma}_{2,s_{t-1}}$	1	-1.921	0.214	[-2.339,	-1.505]	2.843	0.627
	2	-0.585	0.204	[-0.981,	-0.190]	1.428	0.797
	3	1.218	0.210	[0.827,	1.645]	2.979	0.706
$\gamma^z_{2,s_{t-1}}$	1	-0.052	0.291	[-0.622,	0.521]	2.126	0.788
	2	-0.165	0.279	[-0.701,	0.392]	1.446	0.919
	3	-0.315	0.288	[-0.870,	0.248]	1.357	0.099
ρ_1		0.183	0.253	[-0.292,	0.667]	8.403	0.399
ρ_2		-0.196	0.190	[-0.545,	0.186]	18.487	0.603
Panel D: State differences in currency-liquidity-timing coefficients							
$\mu_2 - \mu_1$		0.206	0.119	[0.174,	0.537]	70.373	0.651
$\mu_3 - \mu_2$		0.144	0.347	[0.024,	1.071]	73.253	0.546
$\lambda_2 - \lambda_1$		1.076	0.287	[0.991,	1.560]	71.958	0.618
$\lambda_3 - \lambda_2$		2.146	0.655	[0.077,	2.365]	73.820	0.562

NOTES: This table presents the posterior summary of the best-fitting state-switching model specification $\mathcal{M}_{3,3}$ with controls for currency liquidity reaction, including the posterior means (Mean), the posterior standard errors (s.e.), 95% highest posterior density interval (95% HPDI), inefficiency factor (Ineff) and Geweke (1992)'s p-value (p-val) of the obtained parameters' posterior samples. The model specification is given by

$$R_t = \alpha + \beta^{\text{HML\_FX}}\text{HML\_FX}_t + \beta^{\text{RX}}\text{RX}_t + \mu_{s_t}\tilde{L}^{\text{Cur}}_t\text{HML\_FX}_t + \lambda_{s_t}\tilde{L}^{\text{Cur}}_t\text{RX}_t + \psi^{\text{HML\_FX}}(L^{\text{Cur}}_{t-1} - \bar{L}^{\text{Cur}})\text{HML\_FX}_t$$
$$+ \psi^{\text{RX}}(L^{\text{Cur}}_{t-1} - \bar{L}^{\text{Cur}})\text{RX}_t + \sum_{j=1}^{J}\beta^j f^j_t + \varepsilon_t,$$

where t denotes a month; $s_t \in \{1, 2, 3\}$ and the associated state transitions are formulated by (5)–(7) of the paper; R_t is the equally weighted return of all sample funds; HML_FX_t and RX_t are the risk factors specific to the currency market—the carry-trade and the dollar factors; $\{f^j_t\}^4_{j=1} = \{\text{GMF}_t, \text{EMF}_t, \text{TERM}_t, \text{CREDIT}_t\}$ are the additional risk factors—the hedged global bond market factor, the emerging bond market factor, the term factor, and the credit factor; L^{Cur}_{t-1} is the one-month lagged systematic currency liquidity and $\bar{L}^{\text{Cur}}$ its historical average; $\tilde{L}^{\text{Cur}}_t$ is the innovation in systematic currency liquidity, obtained from an AR(2) process and represents the unpredictable component of systematic currency liquidity; μ_{s_t} and λ_{s_t} are currency-liquidity-timing coefficients; $\psi^{\text{HML\_FX}}$ and ψ^{RX} are currency-liquidity-reaction coefficients. Results are based on a simulation-based Bayesian inference procedure with 12,500 iterations. The sample period spans from July 2001 to December 2020.

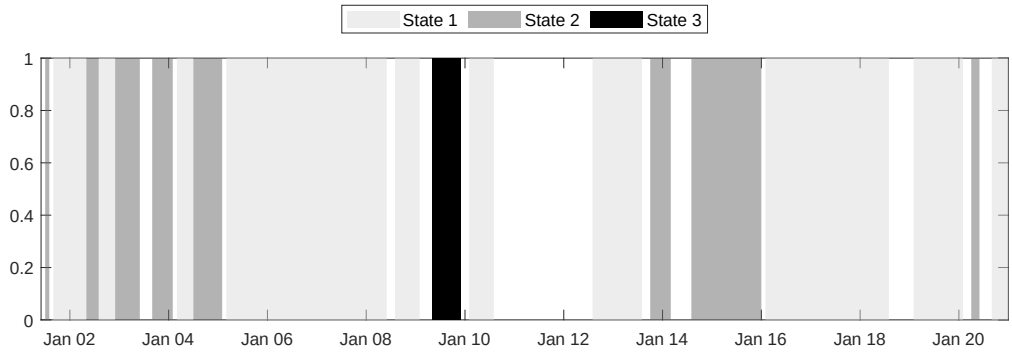

(a) Robustness 1

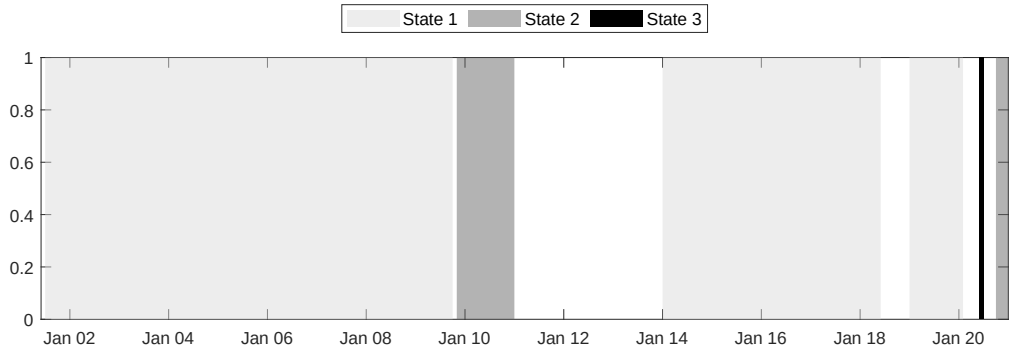

(b) Robustness 2

Figure C.1: Time path of the model-implied three states obtained from the best-fitting state-switching model specification $\mathcal{M}_{3,3}$ with different controls. Each figure plots the shaded areas that highlight the periods of sample funds being in a particular model-implied state. Specifically, the light gray, dark gray, and black areas highlight respectively the periods of sample funds being in the model-implied states $s_t = 1, 2, 3$. The white area highlights the periods during which the model-implied states can not be determined as the probability of each state is less than a threshold of 50%. The sample period spans from July 2001 to December 2020.

References

Chib, S., Jeliazkov, I., 2001. Marginal likelihood from the Metropolis–Hastings output. Journal of the American Statistical Association 96, 270–281.

Geweke, J., 1992. Evaluating the accuracy of sampling-based approaches to the calculations of posterior moments. Bayesian Statistics 4, 641–649.

Hwu, S.T., Kim, C.J., Piger, J., 2021. An N-state endogenous Markov-switching model with applications in macroeconomics and finance. Macroeconomic Dynamics 25, 1937–1965.

Kim, Y.M., Kang, K.H., 2022. Bayesian inference of multivariate regression models with endogenous Markov regime-switching parameters. Journal of Financial Econometrics 20, 391–436.

Menkhoff, L., Sarno, L., Schmeling, M., Schrimpf, A., 2012. Carry trades and global foreign exchange volatility. The Journal of Finance 67, 681–718.